Materials Horizons

Emerging Iongel Materials Towards Applications in Energy and Bioelectronics

Journal:	*Materials Horizons*
Manuscript ID	MH-REV-08-2021-001263.R1
Article Type:	Review Article
Date Submitted by the Author:	30-Sep-2021
Complete List of Authors:	Mecerreyes, David; University of the Basque Country, Polymeric Materials Tomé, Liliana; Universidade Nova de Lisboa, Instituto de Tecnologia Química e Biológica António Xavier Porcarelli, Luca; Deakin University, Institute for Frontier Materials; University of the Basque Country, Polymat, Institute for Polymer Materials Bara, Jason; University of Alabama, Chemical & Biological Engineering; www.ua.edu Forsyth, Maria; Deakin University, Institute for frontier Materials

Materials Horizons

REVIEW

Emerging Iongel Materials towards Applications in Energy and Bioelectronics

Received 00th January 20xx,
Accepted 00th January 20xx

DOI: 10.1039/x0xx00000x

Liliana C. Tomé,*†[a] Luca Porcarelli,[a,b] Jason E. Bara,[c] Maria Forsyth,[a,b,d] and David Mecerreyes*[a,d]

During the past two decades, ionic liquids (ILs) have blossomed as versatile task-specific materials with a unique combination of properties, which can be advantageously used in a plethora of different applications. The additional need of incorporating ILs into solid devices led to the development of a new class of ionic soft-solid materials, named here iongels. Nowadays, iongels cover a wide range of materials mostly composed by an IL component immobilized within different matrices such as polymers, inorganic networks, biopolymers or inorganic nanoparticles. This review aims at presenting an integrated perspective on the recent progress and advances in this emerging type of materials. We provide an analysis of the main families of iongels, and highlight the emerging types of these ionic soft materials offering additional properties, such as thermoresponsiveness, self-healing, mixed ionic/electronic properties, (photo)luminescence, among others. Next, recent trends on additive manufacturing (3D printing) of iongels are presented. Finally, their new applications open in the areas of energy, gas separation and (bio)electronics, are detailed and discussed in terms of performance, underpinning it to the structural features and processing of iongel materials.

1. Introduction

Gels are known as soft-solid, jelly-like materials that do not flow.[1] They can be classified as hydrogels, mostly composed by water,[2] or organogels mostly composed by an organic solvent.[3] In the last years, ionogels or ion gels were proposed as an intermediate type of gel where the main component is an ionic liquid (IL), instead of water or an organic solvent. Ionic liquid-based gels show some similarities to hydrogels because of their ionic nature and to organogels due to their nature and composition. Nonetheless, the ion gels possess a unique combination of properties not seen in hydrogels or organogels.

Since the first report on ion gels by Watanabe and coworkers in 2005,[4] there have been plenty of works reported in the literature dealing with these ionic soft solid materials.[5-11] The first observation is that there is not a common name in the literature to refer to gels based on ILs. Many naming systems have been simultaneously adopted, making this a difficult subject to reference. The most common names are ionogel, ion gel, ion-gel, iongel and ionic liquid gels. Throughout this review, we will use the term iongel due the simplicity of its spelling and the pronunciation benefits. The second observation is that the iongel family includes materials with notable diversity of chemical compositions and combination of components. On the one hand, there are numerous ionic liquids based on the high number of combination of cations and anions available.[12] Novel ILs are designed daily, and new ionic compounds, such as protic ILs[13] or deep eutectic solvents (DES),[14] continue to be discovered. On the other hand, it is possible to form a three dimensional network using different type of gelators, namely linear or polymer networks, block copolymers, supramolecular compounds, biopolymers, small molecular weight gelators, organosilane networks or inorganic nanoparticles, among others. All the variables regarding different ILs and gelators, makes that under the name of iongels there is a myriad of diverse soft materials with varying composition and properties, such as mechanical, electronic, chemical or electrochemical. The third observation is that iongels have being successfully tested in many applications ranging from batteries,[15] supercapacitors [16], fuel cells,[17] catalysis,[18] analytical chemistry,[19] gas separation membranes,[20] biosensors,[21] transistors[22] or electrodes[23] in bioelectronics. For each application, the requirements are very different. Thus, the best iongel does not exist and it definitely depends of the property requirements for each application.

In this review, we primarily analyse the main soft ionic materials covered under the umbrella of iongels, ionogels or ionic gels. Next, we will focus on the emerging types of iongels that present additional properties to those typically associated with ILs, such as ionic conductivity, thermal stability, gas solubility or electrochemical widow. The emerging iongels present properties such as thermoresponsiveness, self-healing, mixed ionic/electronic conductivity, superelasticity or (photo-

[a] POLYMAT, University of the Basque Country UPV/EHU, Avda. Tolosa 72, Donostia-San Sebastian 20018, Gipuzkoa, Spain.
[b] Institute for Frontier Materials, Deakin University, Geelong, VIC 3217, Australia.
[c] University of Alabama, Department of Chemical & Biological Engineering, Tuscaloosa, AL 35487-0203 USA.
[d] Ikerbasque, Basque Foundation for Science, 48013 Bilbao, Spain.

† Present address: LAQV-REQUIMTE, Chemistry Department, NOVA School of Science and Technology, Universidade Nova de Lisboa, 2829-516 Caparica, Portugal

electro)luminescence properties. Another important goal of this review is to highlight the emerging trends on advanced processing methods such as additive manufacturing or 3D printing. Finally, the design versatility towards the applications of iongels in areas of energy and (bio)electronics will be highlighted.

2. Chemistry of iongels

2.1 Ionic liquids

In the last two decades, the unique properties of ILs, namely low volatility, thermal stability, ionic conductivity and electrochemical stability, have been advantageously used in a vast number of different applications across all technological fields. However, the greatest feature of ILs is perhaps their designer nature.[12] Nowadays, one can find a wide range of functional ILs with completely different properties. For instance, ILs can be acidic or basic, hydrophobic or hydrophilic. Some ILs are very expensive, some others are commodities with low cost. In some cases ILs can be biocompatible in others have toxic tendencies or cause environmental damage,[24] while others are made from renewable resources,[25] and designed to be biodegradable.[26] Some ILs are able to dissolve cellulose[27] or to kill microbes[28] and bacteria,[29] others have functional pharmaceutical therapeutic qualities.[30] ILs can be designed as excellent battery electrolytes[31] or as alternative solvents for CO_2 separation processes.[32] It is evident from literature that, the optimum IL chemistry can be vastly different for each application. Some examples of ILs, as well as protic ILs and DES, that have been used to create diverse iongel materials, are presented in Fig. 1.

In the last few years, there have already been excellent reviews in the area of ILs for different applications.[31-39] For this reason, in this review we will not discuss in detail the IL component of the iongels. Only in the last section, we will highlight the main IL components for each particular application along with the remaining challenges. Herein, we remark on some general trends relating to ILs, which have been observed under the umbrella of iongel materials:

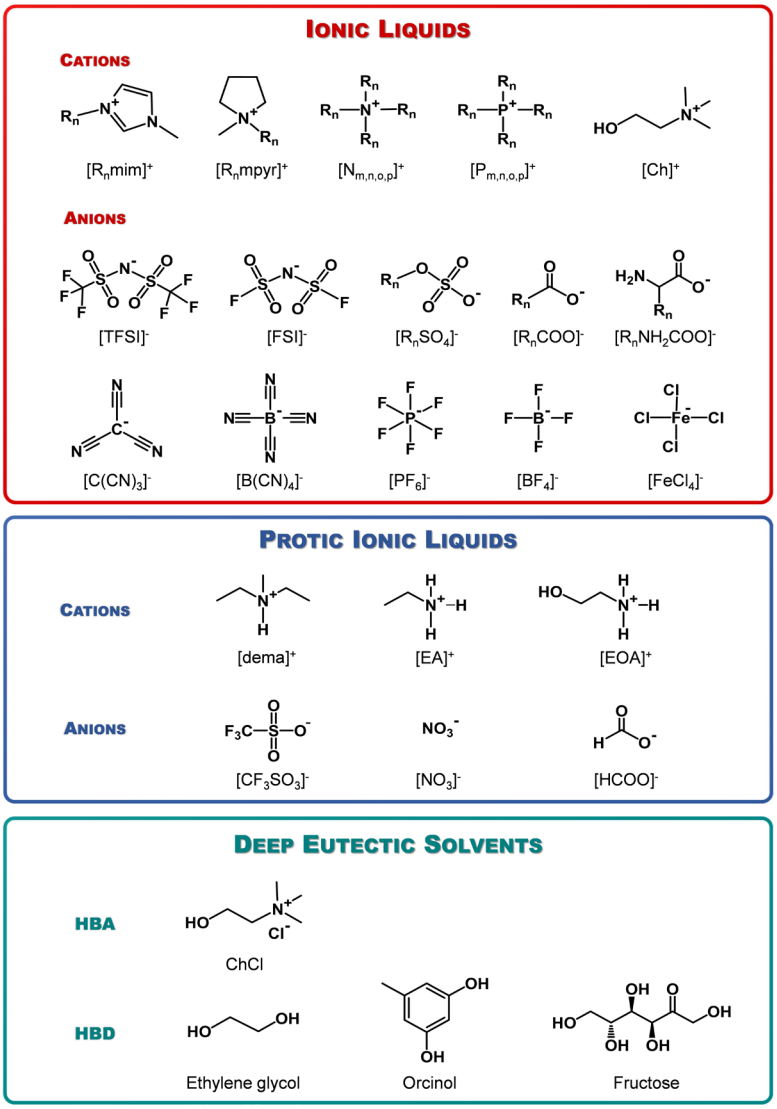

Fig. 1 Chemical structures and abbreviations of a selection of ILs (top), protic ILs (middle) and DES (bottom) used to create diverse iongel materials.

(1) The main driving force behind the development of iongels is to have a material with the properties of an IL, and the mechanical properties and processability of a solid. For this reason, iongels are usually designed using as the main component the highest performing ILs for each specific application.
(2) Occasionally, the liquid phase of iongels includes one IL and a second (and possibly third) component. For instance, in the case of iongels for batteries, the liquid phase of the iongel is formed by a mixture of IL and a Li^+ or Na^+ salt. In other cases, the additional component may be a fluorescent, biologically active or electrochromic compound.
(3) Most of the iongels have been designed using the common ILs used in electrochemistry having imidazolium, pyrrolidinium or phosphonium cations combined with fluorinated based anions such as $[TFSI]^-$ and $[FSI]^-$. Nevertheless, there are numerous of emerging ionic liquids and new ionic compounds, including protic ILs or DES, which are yet to be exploited for the design of iongels.

2.2 Types of gelators

Different types of gelators have been demonstrated to be effective in iongel formation, as schematically illustrated in Fig. 2. These include polymer networks, block copolymers, biopolymers, small molecular weight gelators, supramolecular gelators, organosilane networks or inorganic nanoparticles. In this sub-section, the main issues, advantages and limitations of each type of gelator will be discussed.

Mixing ILs with polymers is the most straightforward strategy to obtain iongels. For instance, Watanabe *et al.*[4] prepared self-standing, flexible and transparent iongels through polymerization of methyl methacrylate (MMA) in $[C_2mim][TFSI]$ IL and a small amount of the cross-linker ethylene glycol dimethacrylate (EGDMA). However, very soon it was realized that the miscibility of ILs with polymers is problematic and dependent on each individual type of IL compound. For this reason, rather than employing commercially available polymers such as poly(methyl methacrylate) (PMMA),[40, 41] poly(vinyl alcohol) (PVA),[42, 43] poly(vinylidene fluoride) (PVDF),[44, 45] or poly(ethylene oxide) (PEO)[46, 47] as gelators, polymeric versions of the ILs named poly(ionic liquid)s (PILs) were used to develop iongels.[48] Here, poly(imidazolium)[49-54] and poly(diallyldimethylammonium)[55-58] type PILs have been the most popular in combination with a variety of counter-anions. However, when mixing high IL contents (on average > 50 wt% depending on the IL/polymer system), the obtained materials do not behave as a gel and are often able to flow. Alternatively, polymer cross-linking methods based on UV-curable resins or thermally curable polymers have been used to develop iongels with high IL content and low polymer gelator content.[59-62] Once more, the main challenge here is to prevent the leaching of the IL in the

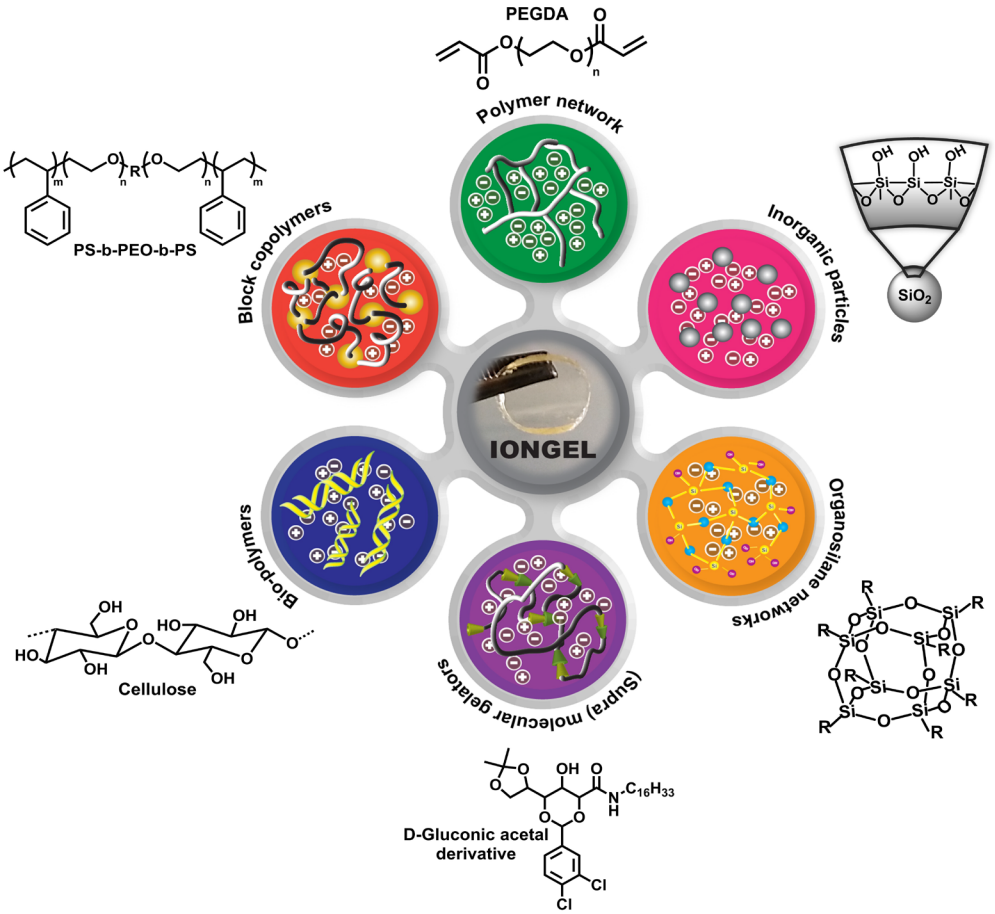

Fig. 2 Schematic representation of different types of iongels and chemical structures of gelators.

iongel. Therefore, ionic polymer networks, which can strongly interact with the IL cations and anions, are preferred.[63-66]

Another gelator type within the synthetic polymer family is the use of block copolymers as pioneered by Lodge *et al.*[67-69] ABA type triblock copolymers are known as good gelators if the 'A' block is insoluble in the solvent, while the 'B' block is soluble. In the case of iongels, the most used ABA triblock copolymers are based on PS-b-PEO-b-PS,[8] since PEO is a relatively IL-philic block and PS is usually IL-phobic. Nonetheless, various ABA type triblock copolymers have recently been synthesized and successfully used to prepare iongels, including polystyrene-b-poly(methyl methacrylate)-b-polystyrene (PSt-b-PMMA-b-PSt),[70] poly(phenethyl methacrylate)-b-poly(methyl methacrylate)-b-poly(phenethyl methacrylate) (PPhEtMA-b-PMMA-b-PPhEtMA),[71] and polystyrene-b-poly(diallyldimethylammonium)-b-polystyrene (PS-b-PDADMA-b-PS).[72] As a drawback, for many types of ILs, the block copolymer has to be specifically designed in terms of composition and chemical nature of the A-B blocks. This fact limits the use of block copolymers due to the need of creating a tailored ABA block copolymer for each type of iongel. Furthermore, the relative amount of IL vs block copolymer is usually limited to a maximum of 80 wt% IL, and over this value, soft materials are typically obtained.

The third type of gelator within the polymer family are biopolymers such as gelatin,[73] agarose,[74] xanthan gum,[75] guar gum,[76] starch,[77] chitosan,[78] or cellulose.[79] Biopolymer gelators have been shown to be very effective especially in the case of hydrophilic type of ILs, such as [C_4mim][Cl], [amim][Br], [C_2mim][Ac], [C_2mim][$EtSO_4$] which interact positively with the biopolymers.[80, 81] However, the biopolymers are usually not a good matrix in the case of iongels based on hydrophophilic ILs for specific applications, where the presence of reactive groups such as amine or hydroxyl may interfere, as for instance in batteries.

The fourth type of gelators and one of the most popular ones are organosilane organic/inorganic networks obtained by sol-gel methods.[82, 83] Le Bideau *et al.,*[84] who proposed the name of "ionogels", pioneered the preparation of soft solids by incorporation of IL in organosilica networks at high IL loadings (97 wt%).[85] The main difficulty here is that the sol-gel method is a reactive process, in which temperature and pH conditions need to be closely monitored and strongly depend on the type of IL. For instance, the sol-gel method should be adapted to each different IL and it is not applicable with some reactive ILs. Furthermore, in order to obtain free-standing and flexible iongels, the combination of organosilane networks with mechanically robust polymer matrices are needed, such as PVDF,[86, 87] or even a poly(diallyldimethylammonium) type poly(ionic liquid).[88]

Inorganic nanoparticles are another popular type of gelator. For example, an iongel can be obtained by dispersing 3 wt% silica (SiO_2) nanoparticles into [C_2mim][TFSI] IL, because of the formation of interconnected particulate silica networks in the IL.[89] Nanoparticles are very powerful gelators and can give rise to iongels with many potential applications.[90-93] However, the iongel formation strongly depends on the size, shape and surface of the inorganic nanoparticle, as well as the chemical nature of the IL component.[94]

Probably the less studied type of gelators are low molecular weight molecules, which induce a physical cross-linking due to non-covalent interactions. Among them, supramolecular interactions such as H-bonding,[95] host-guest chemistry,[96] π-π stacking,[97] metal-ligand coordination,[98] electrostatic,[99] or hydrophobic interactions,[100] are commonly used. Although low molecular weight gelators are particularly specific, they are also very interesting to impart additional properties to the iongels, such as thermoresponsiveness[101] or self-healing,[102] as will be discussed in a subsequent section. Another advantage of these gelators is the fast preparation and processing of the iongels.

2.3 Conventional properties of iongels

Iongels usually preserve the intrinsic IL properties. As mentioned before, the gelator forms the three-dimensional network within the IL and is the responsible for the solid-like gel behaviour. The iongel properties can be tailored by varying the IL and gelator chemical structures, the proportions amid them, and their interactions (covalent vs non-covalent). Amongst the diverse iongel properties, the main ones are the ionic conductivity, selectivity towards CO_2, and the mechanical and rheological properties. It should be pointed out that those properties have been already discussed in previous reviews[10, 38, 103-105] and will be only briefly mentioned here.

The high ionic conductivity is a very attractive property of iongels. Adjusting the composition of the IL and the gelator in the iongel can easily control the ionic conductivity. As illustrated in Fig. 3**a**, increasing the amount of the ionic liquid electrolyte (ILE), enhance the ionic conductivity of the iongels, near to the value of the neat ILE.[106]

Another attractive property of iongels is their high carbon dioxide (CO_2) solubility over light gases such as methane (CH_4), hydrogen (H_2), or nitrogen (N_2) that is illustrated in Fig. 3**c**. This property is especially important for membrane-based CO_2 separation applications.[107-109] In this context, iongel materials enable the IL functionality to be used by providing solid structures whilst retaining liquid-like gas transport properties.[20] Depending on the chemical nature of the IL and gelator, and their respective contents, it is possible to fabricate iongels with gas separation performances similar to their liquid counterparts.[108]

The mechanical and rheological properties of iongels are also key features to consider depending on the application. For instance, in lithium batteries, the Young modulus of the iongels is an important parameter to try to limit the detrimental formation of lithium dendrites. In the case of gas separation membranes, mechanical stability is also a key parameter in long-term operational stability, particularly at high temperatures and pressure gradients, which can limit the practical application of iongel membranes.

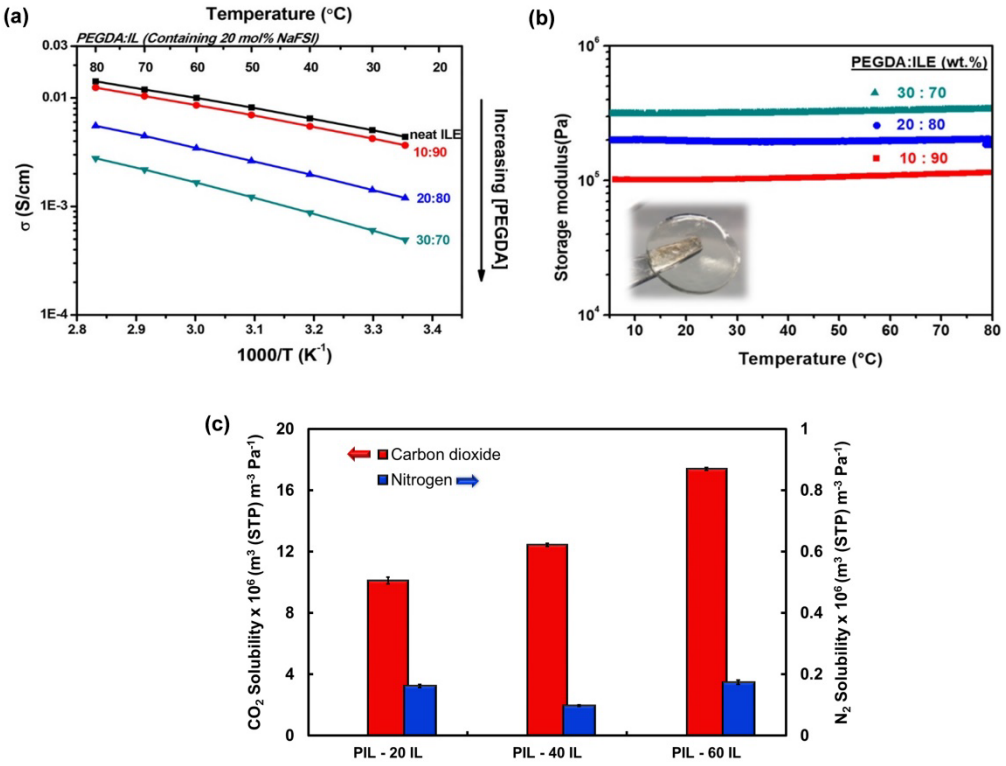

Fig. 3 (a) Ionic conductivity and (b) DMTA analysis vs temperature of iongels containing PEGDA and 90, 80 and 70 wt% ILE ([C_3mpyr][FSI] IL and NaFSI salt). Adapted with permission from Fdz de Añastro *et al.*[106] Copyright 2019, American Chemical Society. (c) CO_2 and N_2 solubilities of iongel membranes prepared with poly(DADMA $C(CN)_3$) (PIL) and 20, 40, 60 wt% [C_2mim][$C(CN)_3$] (IL). Adapted with permission from Tomé *et al.*[110] Copyright 2015, Elsevier.

Overall, the chemical structure of both IL and gelator, as well as the proportion between them, are key factors that affect the mechanical and rheological properties of iongels. As an example, Fig. 3**b** displays the dynamic mechanical thermal analysis (DMTA) of iongels consisted of poly(ethylene glycol) diacrylate (PEGDA) as polymer network and an ILE containing NaFSI salt dissolved in [C_3mpyr][FSI] IL.[106] The storage modulus significantly decreases when increasing the amount of ILE and soft materials are obtained. This is mainly due to a decrease in the network density, as the PEGDA content into the iongel decreases from 30 to 10 wt%. From Fig. 3**b**, it can also be observed that the storage modulus is practically constant between room temperature and 80 °C, meaning that the rubber-like behaviour is preserved and the solid-state structures of the iongels are not destroyed. This demonstrates that cross-linked PEGDA iongels maintain their mechanical properties at different temperatures, which is particularly interesting not only for battery applications,[106] but also for gas membrane operation.[111]

Additionally, the effect of the IL chemical structure on the mechanical and rheological properties of iongels has also been addressed using different types of gelators.[112-116] For instance, Tamate *et al.*[117] recently studied the influence of IL cation and anion on the viscoelastic properties of iongels based on jamming and H-bonding of diblock copolymer micelles in IL. The results showed that when the hydrogen bonding ability of the IL becomes very weak, for example, when a methyl group is present at the C(2) position of imidazolium ring, macroscopic phase separation occurs due to strong H-bonding between the diblock copolymer micelles, resulting in opaque and fragile iongels. Conversely, when the H-bonding ability of the ILs is relatively strong, as the case of [C_2mim][(MeO)HPO_2], the H-bonding among the micelles is significantly suppressed, resulting in lower storage and loss moduli values [117]. Control of competitive H-bonding interaction between polymers and ILs is thus crucial to obtain the desirable mechanical properties. Furthermore, Brogan *et al.*[118] systematically explored the stress-strain relationships of iongels containing cross-linked PEGDA and ILs with different anion basicity (β). The results showed that the strength of iongels is inversely related to the IL anion polarity. The better solvents for PEGDA were the less polar ILs, ensuing iongels with improved strength and toughness.[118]

Unfortunately, there has not been any study that compares the mechanical properties of different iongels having the same IL component and different gelators at the same ratio. Here, intuitively, it is expected that inorganic particles or aromatic compounds lead to iongels with superior Young modulus.[103]

2.4 Iongels with "additional properties"

In the last years, a great amount of work has been devoted to preparation of iongels with additional properties besides those

discussed in the previous section. As shown in Fig. 4, a large variety of emerging iongels have been synthesized showing new functionalities in addition to the conventional properties of iongels (ionic conductivity, thermal, electrochemical). This has led to a new generation of iongels with unique mechanical properties such as self-healing, stretchability, shape memory or hyperelasticity. Responsive iongels, demonstrating thermo- or photo-responsiveness, have also been very extensively researched. More recently, other attractive properties have also been added to the iongel materials portfolio, including mixed ionic/electronic conductivity, luminescence, magnetism, biocompatibility and bioactivity. In this section, we will highlight some examples of these emerging iongels showing additional properties or functionalities.

Fig. 4 Pictures of emerging iongels with additional properties or functionalities. Adapted with permission from (a) Noro *et al.*[119] Copyright 2013, American Chemical Society. (b) Li *et al.*[120] Copyright 2019, American Chemical Society. (c) D'Angelo *et al.*[121] Copyright 2019, American Chemical Society. (d) Tamate *et al.*[102] Copyright 2018, John Wiley and Sons. (e) Del Água *et al.*[122] Copyright 2017, American Chemical Society. (f) Ziółkowski *et al.*[123] Copyright 2012, John Wiley and Sons.

Iongels can show interesting thermoresponsive behaviour (Fig. 4a). In this case, the mechanical/rheological properties,[119] swelling degree or volume[124] of iongel change reversibly with the temperature. These iongels can be used in different applications, namely reversible water uptake, actuators, or flexible optical devices.[125] In a typical example, iongels formed by inorganic nanoparticles and ILs are in the gel state at room temperature, but they able to flow at high temperature showing a fluid-like behaviour. In this case, the iongel show a gel-sol transition temperature typical of many types of supramolecular gelators. This property can be advantageously used to process iongel materials by advanced methods, such as 3D printing, as will be discussed in the next section. On the other hand, iongels can also unveil thermo-responsive behaviour as other type of poly(*N*-isopropylacrylamide), i.e. PNIPAM gels, which can be swollen or collapsed reversibly with temperature. Benito-Lopez *et al.*[124] showed that an iongel consisting of $[C_2mim][EtSO_4]$ and cross-linked PNIPAM can be used as a thermoresponsive valve in microfluidic devices taking advantage of this property. The use of gelators or ILs

comprising photosensitive moieties has also been reported as a straightforward strategy to prepare photo-responsive iongels.[71, 126-128]

Luminescent iongels have been prepared by adding a number of organic and inorganic luminescent dyes to iongels. For instance, Lunstroot *et al.*[129] reported an imidazolium-based IL with an europium (III) tetrakis β-diketonate complex confined in a silica network. The resulting materials revealed intense red photoluminescence under UV irradiation. Moreover, the same authors have described the first lanthanide-containing luminescent iongels based on a polymer matrix.[130] Highly luminescent and flexible iongel films were obtained by incorporating europium (III) complexes in the PMMA/[C_6mim][TFSI] matrix. Later on, Xie *et al.*[131] developed iongels with a chromophore of platinum and europium bimetallic complex. The chromophore was combined with PMMA and [C_4mim][TFSI], yielding transparent, flexible, ion conductive, and luminescent iongels, which are interesting candidates for soft organic light emitting diodes. More recently, Li *et al.*[120] prepared luminescent iongels (Fig. 4**b**) by mixing sodium deoxycholate and europium nitrate in a protic IL ([EA][NO_3]). In comparison to other lanthanide-iongels, typically obtained by doping lanthanides in ILs, polymer matrices or solid supports, the sodium deoxycholate-based iongels were straightly built into nanofibers by metal coordination and hydrogen bonding. These reports demonstrate that luminescent iongels with enhanced mechanical properties hold great potential for applications in the fields of solid electrolytes, biosensors and optical devices.

Iongel materials showing shape-memory and self-healing properties (Figs. 4 **c** and **d**,) are also of particular interest. To illustrate with some recent examples, Li *et al.*[132] reported such behaviours in a iongel supported by a silicone backbone containing [C_2mim][TFSI] and tannic acid. Singh *et al.*[133] also observed that an iongel formed from [C_2min][$EtSO_4$] and gelatin showed highly stretchable and self-healing behaviour, while an analogous gelatin-based hydrogel did not. Trivedy *et al.*[134] also reported an agarose-based iongel with self-healing properties. On the other hand, synthetic supramolecular polymers have also been explored as gelators in the preparation of iongels with self-healing properties. For instance, the use of gelators based on D-gluconic acetal derivatives[97] or PILs having ureido-pyrimidinone (UPy)[135] with dynamic cross-linking points resulted in iongels displaying self-healing behaviour. In general, shape memory and self-healing properties are usually boosted through multiple forms of non-covalent supramolecular interactions,[136] namely H-bonding and coulombic forces, between the IL and gelator.

Conducting polymer hydrogels are driving increased attention because of their ability to conduct both electrons and ions.[137, 138] Nevertheless, conducting polymer hydrogels suffer water evaporation that results in the loss of mechanical stability and conductive properties. Recently, del Agua *et al.*[122] reported a conducting iongel (Fig. 4**e**) formed by guar gum, poly(3,4-ethylenedioxythiophene) (PEDOT) and [C_4mim][Cl] IL. A unique combination of properties was obtained in this iongel material that includes the electronic conductivity of PEDOT, the support and flexibility given by guar gum, as well as the ionic conductivity and negligible vapour pressure of the IL. Nowadays, the development of conducting polymer type iongels is a very active field of research because of the interesting mixed ionic/electronic conductivity and the potential use of these materials as sensors and electronic skin in bioelectronics.[139, 140]

Iongels presenting magnetic properties can be classified in two types, depending on the material that generates the magnetic properties. First, paramagnetic iongels have been developed based on ILs containing paramagnetic anions such as $[FeCl_4]^-$.[141] The resulting iongels were transparent, flexible, and combined the paramagnetic functionality of the metal-IL with mechanical properties of the matrix. Second, magnetic iongels have also been prepared using magnetic nanoparticles as gelator,[142] or by introducing iron oxide (Fe_2O_3) nanoparticles into a typical iongel formulation including ILs and a polymeric gelator.[123] These iongels respond to external permanent magnets (Fig. 4**f**) and thus, they are promising materials for new soft magnetic actuators.

During the past few years, due the increasing demand of soft ionic materials, considerable research efforts have been made in the development of iongels showing biocompatibility, biodegradability and bioactive properties (Fig. 4**g**). In the first case, the most investigated iongel types have been those that include biocompatible ILs, such as the ones based on cholinium, and gelators of biocompatible synthetic polymers or natural biopolymers. As an example, Isik *et al.*[143] proposed a series of biocompatible iongels by trapping cholinium lactate ILs into methacrylic polymer networks. Later on, Yuen *et al.*[144] reported the use of polycarbonate networks as gelators to form iongels that were hydrolytically degradable. This function allowed for the possibility of having biodegradable iongels. Furthermore, Jo *et al.*[145] recently suggested a biocompatible and biodegradable iongel composed of cholinium malate and levan polysaccharide. On the other hand, in order to produce soft solid materials with excellent antibacterial properties, bioactive iongels have been prepared by incorporation of bioactive cholinium-based ILs having carboxylate[29] or amino acid[146] anions into polysaccharides, such as chitin, chitosan or cellulose.

3. Advanced processing methods

Because iongels contain ILs (which can have essentially zero vapour pressure) they are not subject to desiccation (i.e., "drying out') and a change in properties over time and temperature as do hydrogels or organogels. This affords advantages in terms of their ability to be processed using both simplistic and sophisticated methods. In this review, we are highlighting some recent examples of advanced processing methods, such as electrospinning, sol-gel techniques, inkjet printing, transfer stamping and 3D printing of iongels (Fig. 5), each of which has relative advantages and disadvantages depending on the desired form of the iongel and the end-use application.

Sol-gel processing methods are typically used to form a network of inorganic oxides such as SiO_2 or TiO_2 and can result in highly porous solids such as xerogels or aerogels after the liquid is removed from the gel via evaporation.[83, 84] However, ILs will not evaporate and will be retained within the inorganic component. Sol-gel processing allows for control over shape, thickness and flexibility of the iongel product.[83, 84, 129, 147] The good solvation power of ILs allows for the inclusion of functional solutes within the iongel, which would not be possible if the liquid was volatile. Some interesting examples have include luminescent lanthanides,[83, 129] photoluminescent polymers,[148] catalysts,[149] and carbon dots.[147] In the case of the carbon dots, control over iongel thickness directly impacted the colour observed.[147]

Relatively stiff, non-crosslinked iongels containing only organic species, such as those produced by Voss *et al.*[150] from

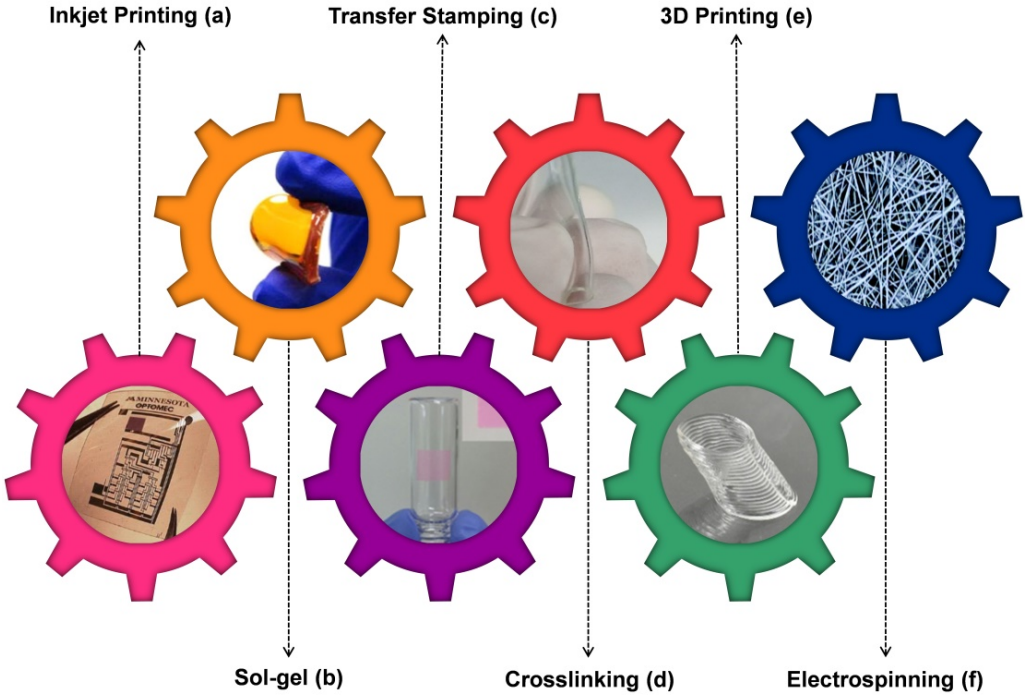

Fig. 5 Iongel materials processed using different methods. Adapted with permission from: (a) Ha *et al*.[151] Copyright 2013, American Chemical Society. (b) Wang *et al.*[147] Copyright 2014, American Chemical Society. (c) Kim *et al.*[152] Copyright 2017, American Chemical Society. (d) Zhong *et al.*[153] Copyright 2018, American Chemical Society. (e) Wong *et al.*[154] Copyright 2019, John Wiley and Sons. (f) Ye *et al.*[155] Copyright 2015, Royal Society of Chemistry.

[C_6mim][TFSI] and gelators such as 12-hydroxystearic acid (12-HSA) can be manually shaped, molded and spread as thin coatings, although they may be easily deformed under applied stress. Relatively complex and large structures of such iongels could be produced through syringe-based 3D printing. Of course, the durability of such printed iongel structures would need to be enhanced through a curing step. In these non-crosslinked iongels formed around gelators, the cooling rate can have an impact on the nature of the self-assembly and mechanical properties. For example, Takeno and Kozuka found that an iongel formed from [abim][TFSI] showed a twisted structure that resulted when a slow cooling rate (0.4 °C/min) was applied.[156] However, spherical domains and a fibrous structure were observed when rapid quenching was applied, thus the processing conditions may be critical to achieving a desired morphology.

Iongels which are more robustly stabilized through the presence of a polymer or crosslinked networks are desirable in many applications. As previously discussed, the use of photocrosslinking techniques is a straightforward method by which to produce mechanically stable iongels. While the predominant use of this technique has been to conveniently produce simple two-dimensional thin films *in situ* for use as polymer-stabilized electrolytes,[157] and gas separation membranes,[158] iongels can be processed into more complex geometries using several techniques.

Zhong *et al.*[153] demonstrated patterning of an iongel prepared via photocrosslinking of PEGDA and a thiol in the presence of [C_2mim][TFSI]. The presence of residual thiol groups resulted in a reactive surface, which could be patterned via photolithography using water as the photoresist developer. This process yields iongels with intricately patterned, three-dimensional microstructures. These processing techniques could enable the production of flexible microdevices for electrochemical applications.

Blade coating and printing are methods that can be used to produce iongel materials dimensions at small length scales.[159, 160] Lodge, Frisbie and co-workers have demonstrated that thermoreversible iongels composed of [C_2mim][TFSI] and a block copolymer can be printed in the liquid state using aerosol jets at elevated temperatures to produce printed circuits on plastic substrates with features as small as 25 μm.[8,

[151, 161] Aerosol jet printing of iongels is viewed as more practical than inkjet printing as it tolerates a wide range of "ink" viscosity. Lodge also points out that simple techniques such as spin-coating and solvent casting are very useful for iongel processing, as demonstrated by the formation of thin films comprising 20 wt% of poly(vinylidene fluoride-co-hexafluoropropylene) (PVDF-HFP) and 80 wt% [C_2mim][TFSI].[151] These iongels can then simply be cut and applied to surfaces,[162] although the overall dimensions (i.e., length, width) of films produced through solvent casting and especially spin coating will be limited to tens of centimeters.

Transfer stamping has also been employed as a method of applying iongels of specific sizes/areas/thicknesses to surfaces. Lee and co-workers have spin-coated an iongel comprised of PVDF-HFP and [C_2mim][TFSI] onto poly(dimethylsiloxane) (PDMS) stamps of various sizes. These iongel-PDMS stamps were then contacted with various flat and curved surfaces and the iongel was partially melted to improve adhesion to the substrate. Upon cooling, the PDMS was peeled away and the iongel transferred. This technique was demonstrated with aluminium, polyimide (PI), poly(ethylene terephthalate) (PET) and glass surfaces.[152, 163] However, this process may require great care and meticulous preparation in order to achieve success.

Electrospinning is a process in which a polymer solution or polymer melt is drawn through a narrow orifice as a response to an applied voltage and electrostatic repulsion. Electrospinning can be used for a wide variety of polymers (both neutral and charged) as well as iongels. Electrospinning of iongels produces non-woven mats of iongel nanofibers in random patterns, which leads to high surface area materials that can be applied to applications such as sensing, catalysis, biomedical and healthcare, to name a few. As a detailed review on electrospinning of iongels was published by Taubert several years ago, the reader is referred to that work for more details on this method.[164] As with the other methods previously described, electrospinning is also limited in terms of the overall throughput of iongel and is limited to perhaps a few grams per hour.

The growth of mask projection stereolithography (SLA) 3D printing will certainly enable iongels to be formed into high-resolution objects of virtually any geometry. Long and co-workers first demonstrated this technique on IL-based substrates through the copolymerization of a phosphonium-based IL monomers with poly(ethylene glycol) dimethacrylate (PEGDMA).[165] While the resulting material did not meet the definition of an iongel as the cationic components were attached to the polymer backbone and there was no "free" IL present, SLA-based 3D printing has recently been extended to iongels. Furukawa and co-workers demonstrated SLA-based 3D printing of complex, high-resolution objects built from an iongel containing [C_4mim][FSI] immobilized by the UV-induced crosslinking of a thiol-ene network.[166] As shown in Fig. 6, freestanding objects of various shapes, sizes and complexity could be printed from the pre-gel solution with rapid curing of the iongel. Features with dimensions as small as 200 μm were achieved.

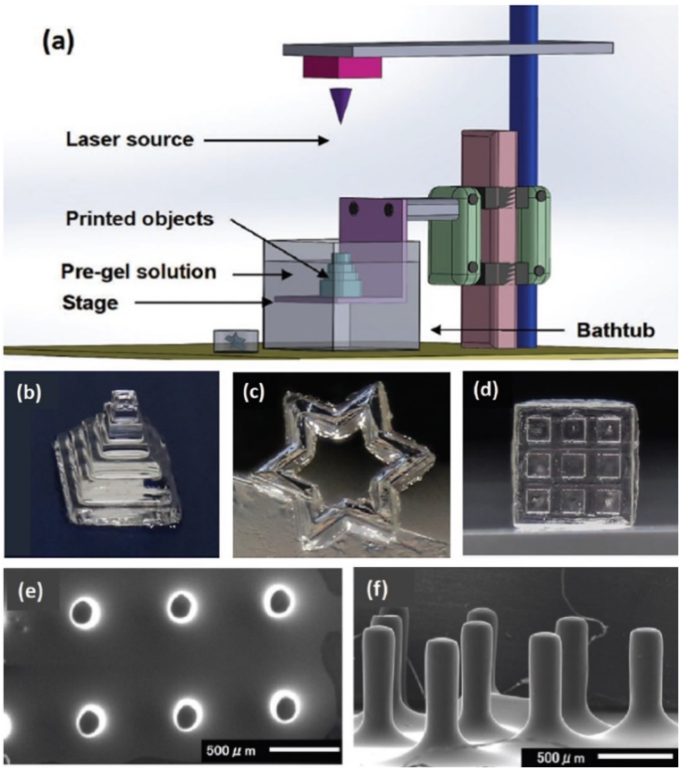

Fig. 6 (a) Schematic of SLA 3D printing of an iongel, (b-d) various printing iongel freestanding objects, (e-f) printed features on the order of 200 μm. Reprinted with permission from Ahmed *et al.*[166] Copyright 2018, John Wiley and Sons.

Additionally, Wong *et al.* used 3D printing and UV curing to produce iongels that were used as strain sensors.[154] Very recently, Luque *et al.* explored the 3D printing via direct-ink writing of thermoreversible iongels by extrusion.[167] In this case, the iongel material had to flow through the nozzle and needed to undergo rapid regelation just after ejection in order to maintain high shape fidelity of the printed structures, which were integrated in different body sensor devices.[167] Amrita *et al.* also used direct-ink write 3D printing to deposit iongel inks and create multimaterial objects that use a single mechanoactivation event to elicit both a mechanochromic response and an autonomous shape change.[168]

Undoubtedly, 3D printing is a versatile and universally accessible technique for processing iongel materials as researchers can now purchase a range of SLA 3D printers at various price points. The growth in 3D printing as a democratized processing tool will undoubtedly lead to more advances in the production of iongel materials and devices. Current 3D printing techniques are unable to produce features at the 1-μm scale, which may be possible with solvent casting or spin coating. However, 3D printing holds significant advantages in terms of automation of the processing and allows for much larger objects and complex designs to be produced than are possible with the other techniques described here which yield 1D (i.e., fibers) or 2D materials.

4. Applications

The recent trends on iongels for emerging technological applications are highlighted throughout the next sub-sections. In particular, real progress has been made on iongels for energy conversion and storage, gas separation and (bio)electronics as illustrated in Fig. 7. Specific and selected examples of iongels are detailed and discussed, including an integrated perspective in terms of performance improvements, underpinning it to the structural features of iongel materials.

As discussed before iongels bring some of the properties of IL to soft solid materials and thus, offer a way to further utilise ILs in solid devices. Many technological applications have the need of circumventing drawbacks related to the shaping and risk of leakage of ILs. This makes that iongels are very popular in final devices/applications, where issues like fabrication and durability are mandatory. Through the next pages, the versatility of iongels will be illustrated showing examples of different iongel materials and their wide range of applications, ranging from solid state batteries (Li, Na), supercapacitors, solar cells, fuel cells, gas separation membranes, bioelectrodes, electronic skin or drug delivery devices.

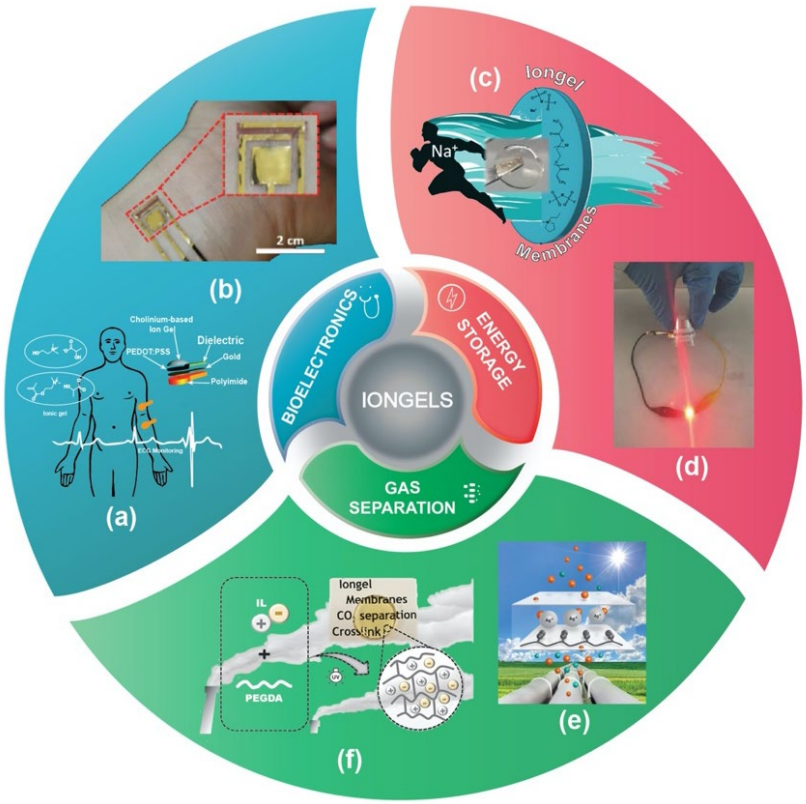

Fig. 7 Perspective of new applications of iongels. (a) Electrodes for cutaneous electrophysiology. Adapted with permission from Isik *et al.*[169] Copyright 2015, Royal Chemistry Society; (b) Organic transistors. Adapted with permission from Jo *et al.*[145] Copyright 2020, John Wiley and Sons; (c) All-solid-state rechargeable sodium batteries. Adapted with permission from Fdz De Añastro *et al.*[106] Copyright 2019, American Chemical Society; (d) Flexible supercapacitors. Adapted with permission from Zhang *et al.*[16] Copyright 2018, John Wiley and Sons; (e) Olefin-facilitated transport membranes. Reprinted with permission from Tomé *et al.*[170] Copyright 2014, Royal Society of Chemistry; (f) CO_2 separation. Adapted from Martins *et al.*[111]

4.1 Energy conversion and storage

Safety and performance are stringent parameters for electrolytes in energy storage and conversion applications. Conventional liquid electrolytes based on organic solvents, *e.g.* mixtures of linear and cyclic carbonates in the case of Lithium ion batteries, are generally volatile and highly flammable. Therefore, complex thermal management is required to operate devices under safe conditions. In contrast, iongels show high thermal stability that not only increases safety but also simplifies device fabrication. For instance, Le Bideau and co-workers described iongels compatible with the reflow soldering process used in electronic circuit fabrication.[171] In addition, a wide electrochemical stability window makes iongels suitable for high voltage applications.[10] Hence, iongels rapidly gained attention for application in next-generation solid state energy storage and conversion technologies, namely lithium and sodium metal batteries, fuel cells, supercapacitors, and dye sensitized solar cells.

Most of the ILs used in iongels for lithium battery applications are based on quaternary ammonium cations, namely tetraalkylammonium, pyrrolidinium or imidazolium types,[5, 172] combined with fluorinated anions, such as $[TFSI]^-$, $[FSI]^-$, $[BF_4]^-$ or $[PF_6]^-$. However, in recent years, new families of IL and ionic compounds are being investigated, such as phosphonium ILs,[173] bisoxalatoborate ILs,[159, 174] solvated ILs,[175] and DES.[176] A wide variety of gelators have been employed including inorganic ones, such as titania or silicon oxides particles,[177] and polymeric ones, such as PVDF-HFP, PEO, PMMA, poly(vinyl chloride) (PVC) and poly(acrylonitrile) (PAN).[178, 179]

Among energy storage devices, solid state batteries with lithium metal electrodes are the technology that may benefit the most from the unique properties of iongels. ILs are widely recognized as promising candidates for lithium metal electrodes. However, IL electrolytes require porous separator and are still affected by the risks of leakage. Iongels could overcome these issues and enable solid-state batteries, as long as an appropriate combination of mechanical properties and high IL loading is achieved. PEO mixtures with pyrrolidinium and imidazolium can be readily crosslinked by means of UV irradiation in the presence of benzophenone.[180, 181] These studies show that chemical crosslinking can be used to prepare mechanically robust iongels with high IL loadings. Iongels are also prepared by mixing ILs with block copolymers having a hard structural domain and a soft ionic-conducting domain, as showed by the pioneering work of Lodge and co-authors.[8] Schulze *et al.*[182] described a nanostructured iongel based on a highly cross-linked PS block PEO matrix comprising and $[C_4mim][TFSI]$/LiMTFSI mixture. In this system, PS plays the role of the high modulus block, whereas the PEO plays the role of the ion-conductive block where most of the IL/salt mixture was concentrated (Fig. 8 a-c). More recently, Goujon *et al.*[183] proposed a block copolymer having a polystyrene block and an intrinsically conductive PIL block, 1-((2-acryloyloxy)ethyl)-3-butylimidazolium bis(trifluoromethanesulfonyl)imide. The block copolymer with $[C_3mpyr][FSI]$/LiFSI showed good ionic conductivity values (7.6×10^{-3} mS cm^{-1} at 50 °C). Kitazawa *et al.* described a series of iongels based on ABA-triblock copolymers,[175] consisting of PS 'A' blocks and PMMA, PEO, and poly(butyl acrylate) (PBA) 'B' blocks. The triblock copolymers were mixed with a Li-glyme solvate IL. These iongels reached (at room temperature) a conductivity of 10^{-4} S cm^{-1} and their electrochemical stability window exceeded 4V. This interesting strategy holds tremendous potential for replacing expensive ILs with cheaper alternative ionic compounds in iongels. In recent years, the use of block copolymers became a viable strategy complementary to chemical crosslinking for achieving iongels with good mechanical properties and high IL loading.

A common issue with high IL loading is the compatibility between the polymer matrix, since poor compatibility can cause the leakage of IL outside the iongel matrix. Poly(ionic liquid)s are very popular gelators for the preparation of iongels due to their excellent chemical affinity with ILs and intrinsic ionic conductivity. In particular, poly(DADMA) is one of the most studied because of its excellent mechanical properties.[184-186] For instance, Zhou *et al.*[187] prepared hierarchical PIL-based iongel electrolyte (HPILSE) based on 1,4-bis[3-(2-acryloyloxyethyl)imidazolium-1-yl]butane bis[-bis(trifluoromethanesulfonyl)imide], $[C_2mim][TFSI]$-based electrolyte and poly(DADMA TFSI). The iongel membrane provided a tensile strength of 2.4 MPa and high ionic conductivity up to 1 mS cm^{-1} at 25 °C. A lithium metal/LiHPILSE/$LiFePO_4$ cell delivered 97.7% capacity retention after 100 cycles at 0.1C with approximately 100% coulombic efficiency (Fig. 8d). Thapaliya *et al.*[188] used a layer-by-layer fabrication method for reinforcing a $[C_4mpyr][TFSI]$-based iongel with lithiated nafion and poly(DADMA) chloride. The reinforced iongels showed increased tensile strength values and ionic conductivities in the range of 10^{-4} S cm^{-1} at room temperature. In addition to polymer gelators, composite or hybrid iongels were investigated to combine high IL loadings and mechanical properties into iongel membranes. For instance, Na *et al.* [189] prepared hybrid iongels for lithium-ion capacitors based on polysilsesquioxane crosslinkers bearing pendant PEO chains and methacryloxypropyl groups. The $[C_4mpyr][TFSI]$ IL was mixed with the polysilsesquioxane crosslinkers and thermally cured, resulting in highly conductive hybrid iongels (0.62 mS cm^{-1} at 30 °C). Interestingly, only 5 wt% polysilsesquioxane crosslinker was used to obtain mechanically stable and leak proof iongels.

Aiming at developing high energy density lithium metal batteries, Chen *et al.*[190] developed an iongel electrolyte by confining $[C_3mpyr][TFSI]$ IL and LiTFSI salt within an bioinspired SiO_2 scaffold. The biomimetic ant-nest architecture showed high ionic conductivity (1.37 mS cm^{-1} at 30 °C), exceptional cycling performance in lithium metal cells with $LiNi_{1/3}Mn_{1/3}Co_{1/3}O_2$ and $Li_4Ti_5O_{12}$ electrodes and long cycling stability (up to 3000 cycles). Similarly, Wu *et al.*[191] confined $[C_2mim][TFSI]$ IL and LiTFSI salt inside a TiO_2 inorganic matrix and tested this iongel in lithium metal/$LiFePO_4$ cells with stable cycling at room temperature.

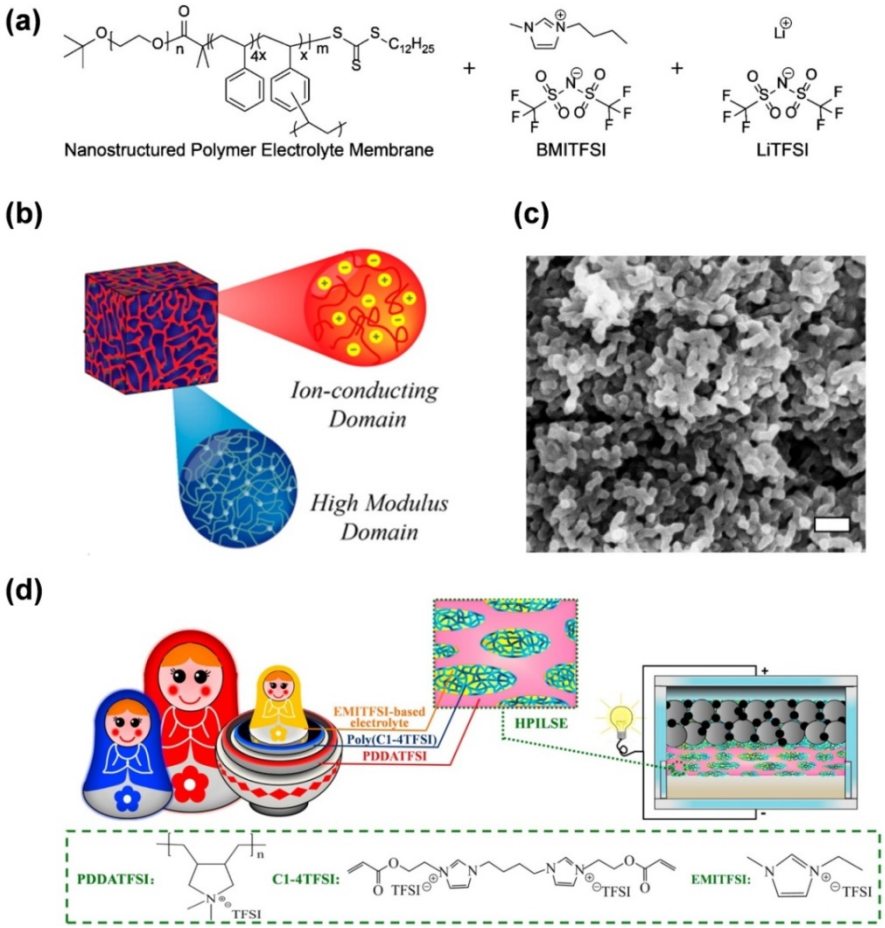

Fig. 8 Iongel-based electrolytes for lithium metal batteries. (a) Chemical structure, (b) schematic illustration and (c) SEM picture of a bicontinuous nanostructure iongels based on 1-butyl-3-methylimidazolium bis(trifluoromethylsulfonyl)imide (BMITFSI), lithium bis(trifluoromethylsulfonyl)imide (LiTFSI) and poly(styrene-block-ethylene oxide). Reprinted and adapted with permission from Schulze *et al.*[182] Copyright 2014, American Chemical Society. (d) Schematic illustration of a hierarchical poly(ionic liquid)-based iongel electrolyte (HPILSE) and its main components. Reprinted and adapted with permission from Zhou *et al.*[187] Copyright 2017, Elsevier.

In recent years, there was a growing interest in post lithium technologies. Among various candidates, sodium ion batteries are the closest to marked readiness. However, sodium ion batteries display lower energy densities than their lithium counterparts. The use of sodium metal electrodes could mitigate this issue if suitable electrolytes for sodium metal are found. This need constitutes an opportunity for the development of sodium conducting iongels. Hashmi and co-workers[192] studied a ternary sodium iongel comprising PVDF-HFP, $[C_2mim][CF_3SO_3]$ IL and $NaCF_3SO_3$ salt, exhibiting ionic conductivities up to 5 mS cm^{-1} at room temperature. Later, it was demonstrated that the addition of $NaAlO_2$ particles slightly enhanced the ion conductivity of the composite electrolyte, where comparable conductivity values were measured in the case of Al_2O_3 particles.[193] Nevertheless, the stable cycling of sodium metal batteries using iongels was only recently demonstrated.[194-196] Mendes *et al.*[197] combined PVDF-HFP, $[C_2mpyr][FSI]$ IL and NaFSI salt into an iongel electrolyte showing excellent performances in a sodium metal/$Na_3V_2(PO_4)_3$ cell operating at room temperature (Fig. 9a-c). Parallelly, Fdz De Añastro *et al.* studied a sodium metal battery with a $NaFePO_4$ cathode operating at 70 °C, the cell comprised a sodium iongel combining poly(DADMA TFSI), $[C_3mpyr][FSI]$ IL and NaFSI salt.[198] The same authors used UV photopolymerization of PEGDA in the presence of $[C_3mpyr][FSI]$ and NaFSI to prepare a mechanically robust iongel that showed ionic conductivity values close to those of the liquid counterpart (7.8×10^{-3} S cm^{-1}) and stable cycling in $NaFePO_4$ metal batteries.[106]

Zinc metal batteries are another interesting post lithium technology that may benefit from the use of iongel electrolytes. Fdz De Añastro *et al.* used a ternary mixture of $[C_2mim][N(CN)_2]$ and $Zn(N(CN)_2)_2$ and poly(DADMA TFSI) showing a high ionic conductivity of 1.1×10^{-2} S/cm^{-1} at 50 °C and wider electrochemical window than its liquid counterpart.[199] Furthermore, iongels were recently applied to lithium sulphur batteries. Baloch *et al.* demonstrated that an iongel coating based on a ternary mixture of poly(DADMA TFSI), $[C_4mpyr][TFSI]$ and LiTFSI salt can delay polysulfide diffusion into the electrolyte and improve performance in lithium sulphur cells.[200]

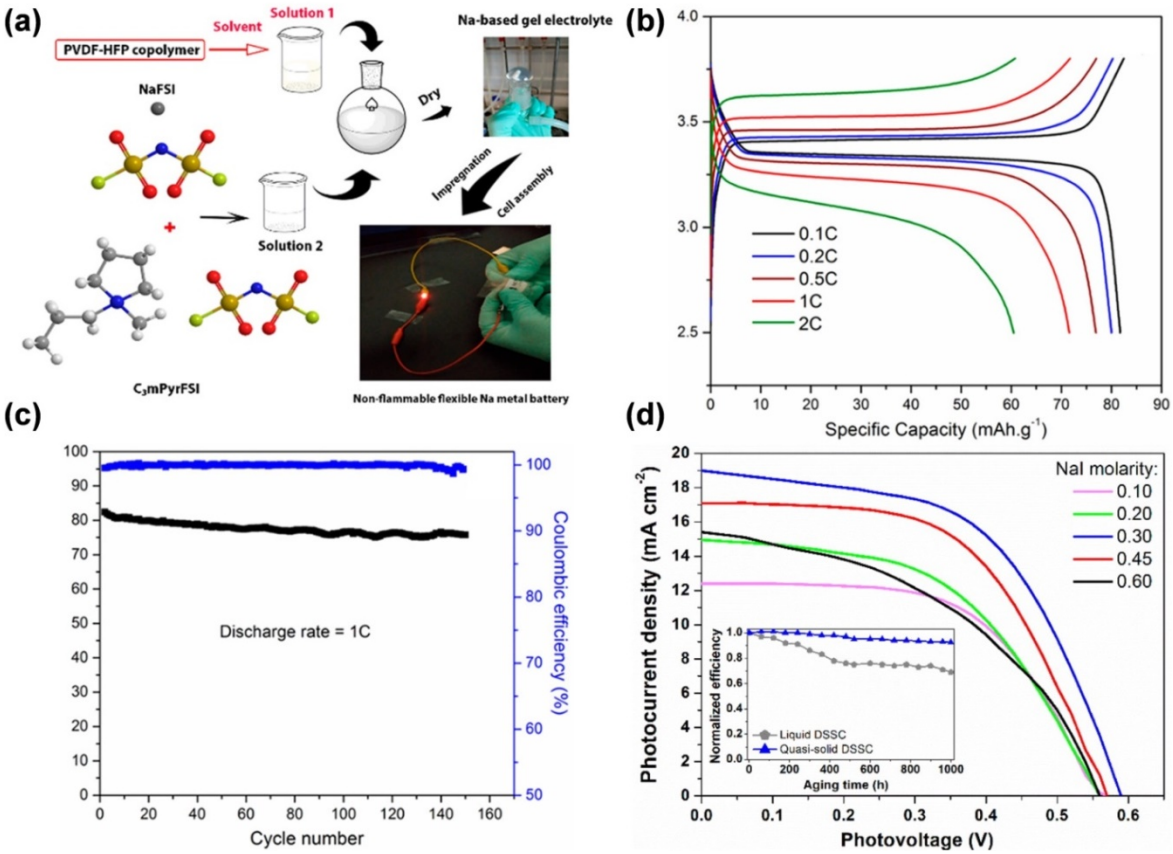

Fig. 9 Iongel-based on PVDF-HFP, [C_2mpyr][FSI] IL and NaFSI for sodium metal batteries (a) iongel chemical structure and preparation schematic, (b) charge and discharge profiles of a sodium metal/$Na_3V_2(PO_4)_3$ battery at different current rates (c) long-term cycling performance of a sodium metal/$Na_3V_2(PO_4)_3$ at fixed 1C-rate for 150 cycles. Reprinted with permission from Mendes *et al.*[197] Copyright 2019, American Chemical Society. (d) Photocurrent curves and power conversion efficiency curve for a dye sensitized solar cell based on PEO, [C_2mim][TFSI] and NaI. Reprinted with permission from Nair *et al.*[180] Copyright 2015, American Chemical Society.

Supercapacitors are energy storage devices with better power density and longer cycle life compared to batteries. Supercapacitors could benefit from iongels in order to increase safety, as well as energy density. For instance, Negre *et al.* prepared SiO_2 matrices in the presence of a IL mixture containing [C_3mpip][FSI] and [C_4mpyr][TFSI],[201] or simply the pure [C_2mim][TFSI] IL.[202] The latter showed a 3 V voltage window which could increase the energy density of the device, high capacitance (between 80 and 90 F g^{-1} at room temperature) and wide operating temperature ranges (−30 to 80 °C). Pazhamalai *et al.*[203] incorporated PVDF-HFP/[N_{2222}][BF_4] iongels into a self-charging supercapacitor based on $MoSe_2$ electrodes and a $NaNbO_3$/PVDF piezoelectric electrospun mat that delivered a specific capacitance of 18.93 mF cm^{-2} when charged at 0.5 mA. However, low temperature performance of iongels is still an issue for developing solid-state supercapacitors despite the larger voltage windows achievable.

Recent studies extended the range of properties and applications of iongels to the preparation of proton conductive membranes. Thus, Chopade *et al.*[204] studied polymerization-induced microphase separation to prepare a proton conducting iongel for application in high-temperature fuel cells. This polymerization method allowed for the creation of a bi-continuous morphology containing PEO/protic IL conducting pathways and cross-linked polystyrene domains. In fact, this approach revealed to be of great promise for the development of highly conductive (14 mS cm^{-1} at 180 °C) and mechanically robust membranes (E = 10 MPa at 180 °C). Kim *et al.*[205] prepared nanophase separated iongels by incorporating a neutral aprotic IL into a poly(styrene sulfonate)-b-polymethylbutylene diblock copolymer. The iongels showed high conductivity values up to 45 mS cm^{-1} in the temperature range between 115 and 165 °C.

Dye-sensitized solar cells (DSSCs) are attracting considerable attention because of their ease of fabrication and low cost. Traditional electrolytes for DSSCs are based on an I^-/I^{3-} redox couple dissolved in volatile organic solvents, which are not practical for long-term operation, due to leakage and evaporation risks. ILs in the form of iongel solid electrolytes could remediate these issues and extend the device life span. Imidazolium type ILs have been extensively used because of their low viscosity in combination with polymeric[206-210] or inorganic[211, 212] gelators. Nair *et al.*[180] reported multifunctional iongels comprising [C_2mim][TFSI] and crosslinked PEO produced by UV polymerization. The iongels were tested in

quasi-solid DSSCs with conversion efficiency exceeding 6% at 1 sun (Fig. 9d). Yu *et al.*[211] proposed a series of iongels based on imidazolium type ILs and different metal oxide nanoparticles. The authors observed increased conversion efficiency produced by the iongels based on TiO_2 particles with respect to the neat ILs, which was attributed to enhanced charge mobility via a Grotthus type mechanism on the surface of the particles.

Materials challenges and perspectives on iongels for energy

Despite iongels shows generally favourable properties, the use of iongels in every day energy devices is still far from market readiness. There are still challenges that the scientific community needs to overcome to turn iongels into a commercial reality. This section aims to highlight these challenges:

(1) Ionic liquids are the most expensive components of iongels due to their limited market demand. At the current stage, iongels are not yet cost competitive in most cases with respect to currently used organic electrolytes and this aspect limits their commercial implementation.

(2) The conductivity of iongels strongly depends on the IL loading, best performances are obtained when the IL loading is higher than 50% wt. However, high loading iongels may lead to soft materials with low modulus as previously remarked.

(3) Iongels usually possess low ionic conductivity with respect to traditional organic electrolytes, as illustrated with an Arrhenius plot in Fig. 10. In some cases, this can reduce the efficiency, safety and life-time in high-density energy storage devices. More work is still required to reach higher ionic conductivity. For instance, the use of superconcentrated ILs might help in mitigating these issues.[213] However, very few reports exist on the use of superconcentrated ILs for iongels and more studies need to be performed in this direction.

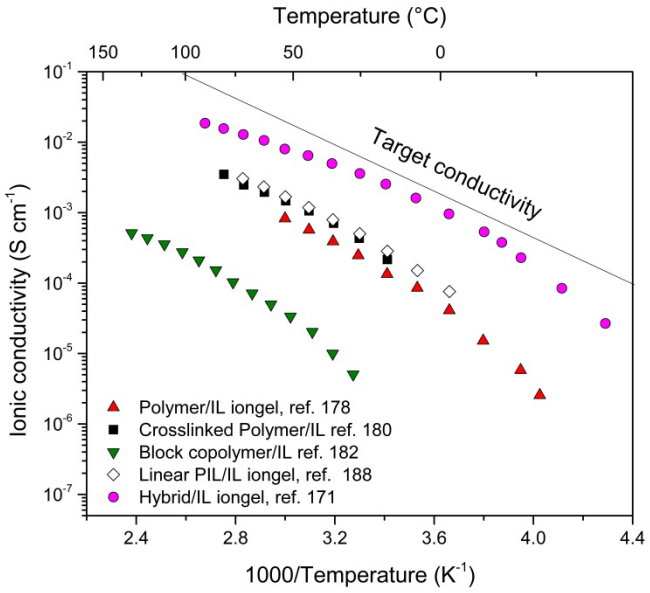

Fig. 10 Ionic conductivity of various iongel families represented on an Arrhenius plot. The solid line is a guide for the eye that represents the target conductivity of iongel electrolytes.

4.2 Gas separation

Ionic liquids for gas separation processes have attracted significant attention during the past two decades, mainly due to their high solubility capacity for gases contained in industrial gas mixtures, such as CO_2, SO_2, H_2S, O_2, hydrocarbons, etc.[214] In fact, CO_2 separation from different point sources is the most studied technology.[107-109] Amongst the different strategies that have been explored towards iongel-based CO_2 separation membranes, the simplest one is the blending of ILs with polymer matrices. Different polymers, such as PVDF,[215, 216] Nafion,[217] Kapton,[218] or Pebax copolymers,[219, 220] have been employed in combination with up to 80 wt% of imidazolium-based ILs bearing $[TFSI]^-$, $[CF_3SO_3]^-$, $[BF_4]^-$ or $[B(CN)_4]^-$ anions.

The development of iongel membranes combining the characteristics of ILs and poly(ionic liquid)s (PIL) has also been conducted,[20] taking advantage of their ability to strongly interact through electrostatic interactions. Bara *et al.* fabricated linear PIL/IL iongels through UV polymerization of imidazolium-based monomers in different type of free ILs.[221, 222] Later on, Tomé *et al.*[110, 223-226] reported another series of linear PIL/IL iongels comprising pyrrolidinium polymer matrices produced by solvent casting. The CO_2 permeability and selectivity of these membranes can be adjusted by varying the amount of IL,[223] using pyrrolidinium random copolymers having anion mixtures,[224] or PIL and IL components bearing different anions,[225] and even by changing the polymer molecular weight.[226] The best performances were achieved with the PIL/IL membranes bearing cyano-functionalized anions, in particular the one containing 60 wt% of $[C_2mim][C(CN)_3]$, that surpassed the Robeson 2008 upper bound (CO_2 permeability of 440 barrer and CO_2/N_2 selectivity of 64).[110] Pyrrolidinium-based PIL/IL systems also been successfully tested for CO_2/H_2 separation in hydrogen purification.[227-229]

Emphasis should also be given to linear PIL/IL iongels using ionic polyimides,[230, 231] due to their excellent mechanical strength and thermal stability. For example, Watanabe and co-workers combined different ILs, namely $[C_4mim][TFSI]$, $[C_4mim][PF_6]$ and $[C_4mpyr][TFSI]$), and sulfonated polyimides (SPI).[232] The highest performance was attained by the $[C_4mim][TFSI]$/SPI iongel (75 wt% IL), with CO_2 permeability of 431 barrer and CO_2/N_2 selectivity of 30, while retaining superior mechanical strength (modulus > 10 MPa) due to the formation of bicontinuous nanostructures of ionic and non-ionic domains. As illustrated in Fig. 11a, the ionic domain consists of the sulfonate structure where the IL is preferentially incorporated and serves as the gas transport path, while the non-ionic domain comprises the aromatic sulfone structure that presents high rigidity and contributes for the mechanical properties. Protic ILs were also employed and their $[N_{124}][TFSI]$/SPI iongels exhibited higher CO_2 permeabilities, though slightly lower CO_2/N_2 selectivities, when compared to aprotic IL ($[N_{1123}][TFSI]$/SPI).[233]

Bara and co-workers have also reported on the synthesis of ionic polyimides and polyamides (PI- and PA-ionene derivatives).[234-236] Interestingly, the thin films (via melt

pressing) of ionic polyimides spontaneously absorb ILs, experiencing an ordering/self-assembly process.[234] Although the CO_2 separation performance of ionene iongels falls short of the CO_2/N_2 and CO_2/CH_4 Robeson 2008 upper bounds, the work developed so far provides a strong foundation to understand structure–property relationships, and in due course produce high-performance membranes.[237, 238]

Cross-linked iongels based on polymer networks have also been intensively investigated during the last few years, because this strategy allows the preparation of membranes with high IL content. Carlisle *et al.*[239] developed cross-linked PIL/IL iongels (≥ 80 wt% [C_2mim][TFSI] IL) with CO_2 permeabilities of 500 barrer and CO_2/N_2 selectivities of 24. Here, the use of a PIL network showed advantages in the fabrication of thin-film composite (TFC) membranes. MacDanel *et al.*[240] used step-growth polymerization to produce epoxy-amine PIL/IL iongels that enable CO_2-facilitated transport (Fig. 11**b**). Under simulated biogas processing conditions, high CO_2 permeabilities (600 – 700 Barrier) an acceptable CO_2/CH_4 selectivities (25 – 35) were obtained.[241] Matsuyama and co-workers focused on the double-network concept (Fig. 11**c**) and reported a tough iongel membrane (80 wt% [P_{4444}][Pro] IL) with outstanding performance for low CO_2 concentration capture.[242] Yin *et al.*[243] fabricated cross-linked PIL/IL iongels via

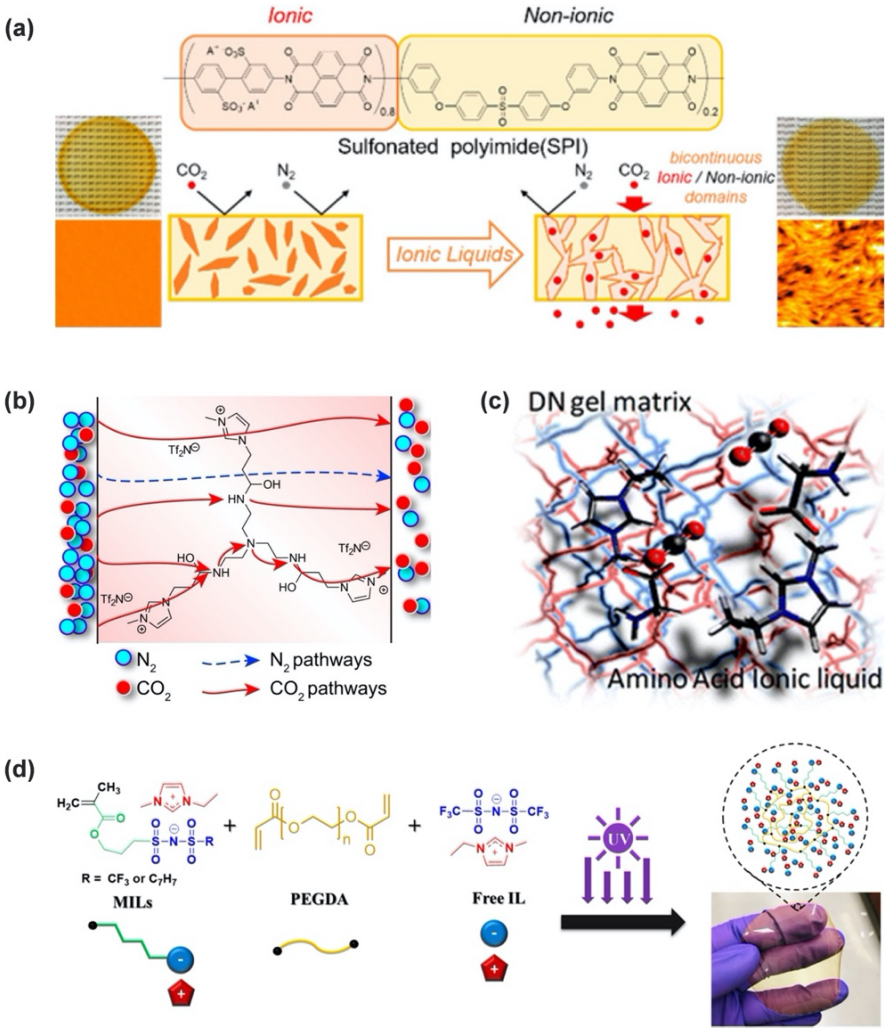

Fig. 11 Iongel-based CO_2 separation membranes. (a) Formation of a bicontinuous nanostructure consisting of ionic and non-ionic domains in IL/sulfonated polyimide iongels. Reprinted with permission from Ito *et al.*[232] Copyright 2018, American Chemical Society; (b) Fixed-site facilitated CO_2 transport through epoxide-amine PIL/IL iongels. Reprinted with permission from Cowan *et al.*[20] Copyright 2016, American Chemical Society; (c) Double-network iongel containing an amino acid IL as the CO_2 carrier. Reprinted with permission from Moghadam *et al.*[244] Copyright 2015, Royal Society of Chemistry; (d) Anionic PIL/IL iongel membranes with cross-linked PEGDA network. Reprinted with permission from Kammakakam *et al.*[245] Copyright 2020, American Chemical Society.

reactions amongst amino-terminated PILs and glycidyl ether crosslinkers. The membrane with 66 wt% [C_2mim][TFSI] IL showed an excellent CO_2 permeability (2070 barrier) but modest CO_2/N_2 selectivity (25). Very recently, Kammakakam *et al.*[245, 246] introduced the first examples of anionic PIL/IL iongel membranes. For instance, as show in Fig. 11**d**, methacryloxy-based IL monomers (MILs), having highly delocalized anions and mobile [C_2mim]$^+$ counter-cations, were successfully synthesized and photopolymerized in the presence of free [C_2mim][TFSI] IL (0.5 and 1 eq.), and an appropriate amount of PEGDA crosslinker (20 wt%) to form flexible and free-standing iongel membranes. The membranes showed CO_2

permeabilities between 5 and 20 barrier, and superior CO_2/N_2 (47 – 87) and CO_2/CH_4 (56-119) selectivities. Nevertheless, the aforementioned cross-linked iongels involve multi-pot procedures and several organic syntheses/purification steps at the monomer level.

Another relevant and simpler strategy is the preparation of iongels in a single-pot using commercially available non-ionic polymer networks. Kusuma *et al.*[247] combined several ILs with PEO/siloxane networks and showed that imidazolium and pyridinium (aromatic cations with acid protons) combined with a low basicity anion ($[TFSI]^-$) imparted more stable membranes. Deng *et al.*[248] used $[C_4mim]^+$ based ILs bearing $[TFSI]^-$, $[BF_4]^-$, $[PF_6]^-$ and $[C(CN)_3]^-$ anions to prepare PEGDA membranes with interpenetrating networks by aza-Michael addition and acrylate homopolymerization. The membrane with 80 wt% $[C_4mim][C(CN)]_3$ IL disclosed 134 barrer of CO_2 permeability and 49.5 of CO_2/N_2 selectivity. Conversely, Martins *et al.*[111] reported an iongel membrane, merely based on PEGDA and 70 wt% $[C_2mim][C(CN)_3]$, with CO_2 permeability of 583 barrer and CO_2/N_2 selectivity of 66, but future improvements regarding mechanical stability should be addressed to circumvent the use of a porous support.

In order to improve the CO_2 separation performance, three-component mixed matrix membranes combining solid fillers, such as zeolites[249, 250] or metal organic frameworks (MOFs),[251, 252] have also been investigated. As an example, Nabais *et al.*[251] incorporated MOFs, i.e. MIL-53(Al), $Cu_3(BTC)_2$ and ZIF-8, into a pyrrolidinium-based PIL/IL (60/40 wt%) matrix. The membrane loaded with 30 wt% MIL-53(Al) showed the CO_2/H_2 selectivity of 13, while that of ZIF-8 revealed a CO_2 permeability of 97 barrer. These PIL/IL/MOF surpassed the upper bound limit for CO_2/H_2 separation.

The CO_2/N_2, CO_2/CH_4 and CO_2/H_2 separation performances of the abovementioned iongels are illustrated in the so-called Robeson plots (Fig. 12), which display solid black lines that represent the empirical upper bounds for each gas pair and illustrate the tradeoff between permeability and selectivity. In brief, strategies such as the use of polymer/IL, linear PIL/IL or cross-linked iongel materials with high IL contents (≥ 60 wt%), have been successfully applied in the preparation of membranes with improved CO_2/N_2 separation performances (Fig. 12**a**). Likewise, the recent advances on ionic polyimide/IL and PIL/IL/porous solid iongels have shown promising results regarding CO_2/CH_4 and CO_2/H_2 gas pairs, with the advantage of improved thermal and mechanical properties in same cases.

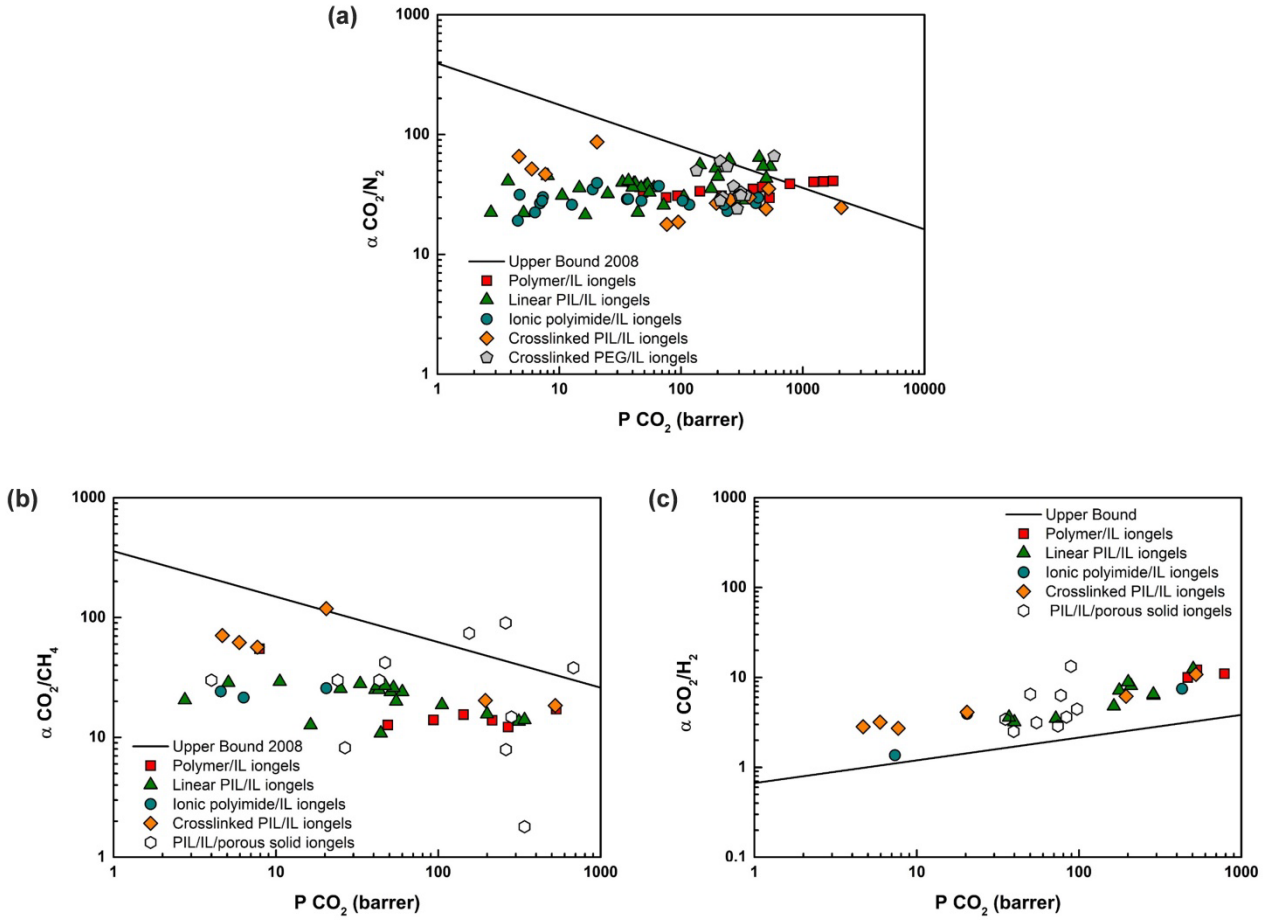

Fig. 12 CO_2 separation efficiencies of iongel membranes represented on (a) CO_2/N_2, (b) CO_2/CH_4 and (c) CO_2/H_2 Robeson plots. Data from refs.[110, 111, 215-218, 220-228, 232-236, 239, 241, 243, 245, 247-252] are illustrated and the upper bounds were adapted from Robeson[253] and Rowe *et al.*[254] Note that the majority of the data points are results of dry single gas studies.

Materials challenges and perspectives on iongels for gas separation

Despite the different polymer and IL features used so far, we underline here on some general trends that have been observed:

(1) As the IL content increases, the CO_2 separation performance of the iongels approaches that of their parent supported IL membranes SLIMs.

(2) High amounts of IL means that the polymer content is rather low and the mechanical stability of the iongels is generally comprised. The need of porous membranes to support the iongels reduce their potential, since the CO_2 performance is limited by the thickness of the support used.

(3) Notwithstanding the great advances in permeability and selectivity, larger permeabilities will be obtained if thin films of iongel materials can be fabricated. Although a detailed work about thin active layers of PIL/IL iongels has been summarized by Noble, Gin and coworkers in 2016,[20] the fabrication of thin-film iongel defect free membranes (ca. 100 nm thick active layer) still constitutes a real challenge in the application of iongel materials for CO_2/light gas separation.

(4) External variables such as temperature, pressure and relative humidity greatly influence the CO_2 separation performance. For instance, in the case of epoxy-amine PIL/IL membranes (Fig. 12**b**), when the CO_2 partial pressure decreases and the relative humidity increases, the CO_2 permeability and selectivity increase due to facilitated CO_2 transport.[240] Nevertheless, there still is a lack of data testing the efficiency of iongel membranes at specific target operating conditions, as well as performing long-term experiments.

4.3 (Bio)electronics

The association of electronics and biology is gaining great interest due to the applications of bioelectronic devices in health monitoring and therapeutics.[139] Nevertheless, developing the next generation of flexible (bio)electronics needs new materials and tremendous efforts have been made in this direction.[255] Organic materials showing ionic/electronic conductivity, flexibility and biocompatibility are urgently needed in this area. Among them, iongels have recently emerged as alternative soft solid materials by virtue of their good ionic conductivity, high mechanical strength, optical transparency and high flexibility.[11] Iongels have been investigated in several applications including devices for electrophysiology, artificial skin devices, sensors and organic transistors.

Iongels are an appealing option for cutaneous electrophysiological recordings since they do not leak or dry out. In this case, Malliaras and coworkers reported iongels-assisted electrodes for long-term cutaneous recordings.[23] Conformal electrodes made of gold and PEDOT:PSS were fabricated and their performance compared in a dry state and in conjunction with an iongel based on [C_2mim][$EtSO_4$] IL and PEGDA. At the interface with human skin, the iongel decreased impedance to levels similar to those of commercial electrodes (1 kHz). The electrode showed this low impedance during 3 days, which makes them appropriate for long-term monitoring of electrophysiological activity.[23]

Following the same research line, Isik *et al.*[169] synthesized cholinium-based iongels through photopolymerization of poly(cholinium lactate methacrylate) network in the presence of [Ch][Lac] IL. These iongels showed good adhesion to the skin and electrocardiography (ECG) signals were recorded with iongel assisted electrodes up to 3 days. The low toxicity of cholinium ILs make these iongels highly attractive for cutaneous electrophysiology.[169] Therefore, Bihar *et al.*[256] used inkjet printing to fabricate PEDOT:PSS electrodes and the contact with the skin was improved using cholinium lactate iongel (Fig. 13a-b). The fully printed electrodes were used to record cardiac activity (Fig. 13c), paving the way for the fabrication of customizable health monitoring devices for cutaneous applications.[256] In addition, Yuen *et al.*[144] prepared biodegradable iongels via ring-opening polymerization of cyclic carbonate monomers within [C_4mim][Lac]. The recorded electrocardiography signals were similar to those of a standard medical electrode. The main advantage of this iongel material is the fast degradability in water at room temperature, that is particularly interesting for implantable electrodes.[144]

More recently, Luque *et al.*[167] designed 3D printable and biocompatible iongels by taking advantage of polyvinyl alcohol/phenol interactions to gelify cholinium carboxylate ionic liquids. These supramolecular cholinium-based iongels showed excellent performance in electrodes for long-lasting ECG recording, until 2 weeks, and the response was comparable to that of commercial medical electrodes.[167] Moreover, Velasco-Bosom *et al.*[257] proposed a new fabrication method to obtain adhesive electrode arrays for cutaneous electrophysiology. The authors developed 4 x 4 array of 1.5 x 1.5 mm^2 electrodes with a center-to-center distance of 3 mm using PEDOT:PSS composite with the [Ch][Lac] IL as electrode, showing an impedance of 2.7 MΩ at 60 Hz. The mm-sized cutaneous arrays recorded high quality spatiotemporal surface electromyography (EMG) maps, allowing to identify the motions of the index, little, and middle fingers, and to directly visualize the propagation of polarization/depolarization waves in the underlying muscles.[257]

Considering the increasing interest in artificial skin devices for application in soft robotics and healthcare, the development of iongels operating in response to diverse human movement has also been expanding in recent years. To illustrate with some examples, Ren *et al.*[258] prepared iongels, using thiol-ene click chemistry under mild conditions. Due to the stretchability and flexibility of the click-iongels, the fabricated triboelectric nanogenerator device exhibited high mechanical stability in a wide operating temperature range (–60 to 200 ºC).[258] Tee and coworkers[259] reported a self-healing PVDF-HFP/[C_2mim][TFSI] iongel, which endured strains as high as 2000 %, for the application of electronic skins operating under water. The authors fabricated a touch, pressure and strain sensor platform to demonstrate the sensory capability

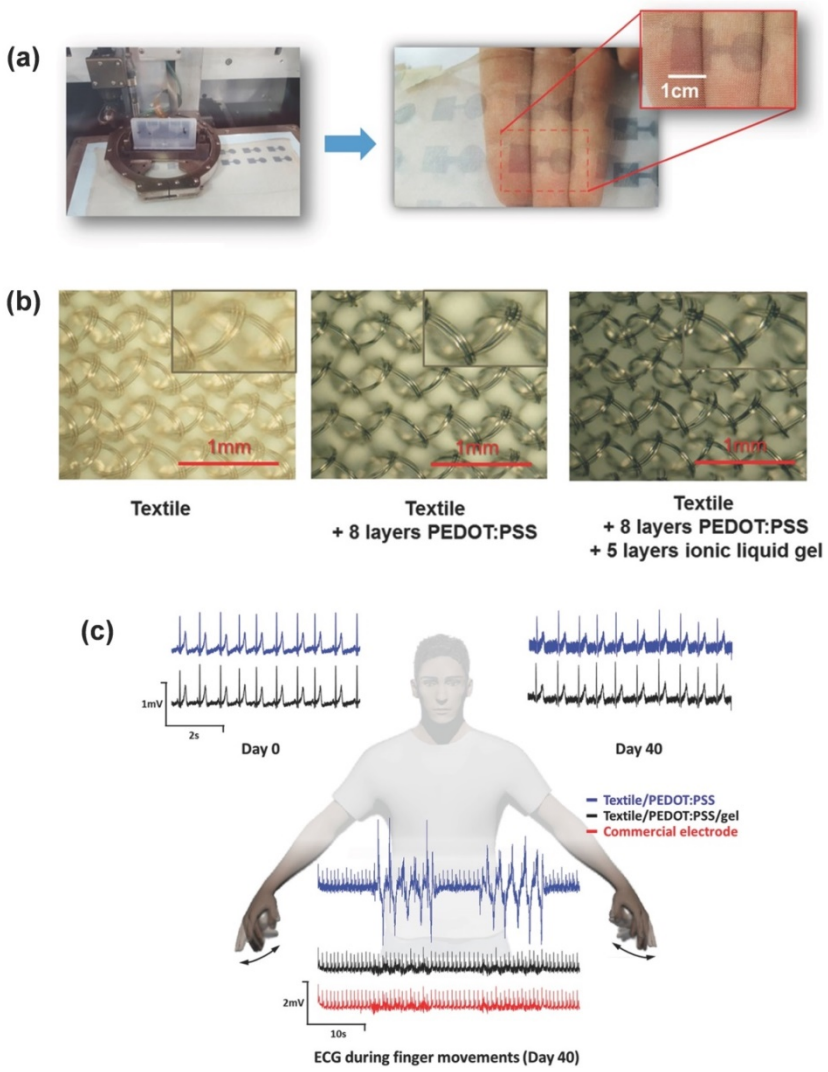

Fig. 13 (a) Photographs of the inject printing process and printed electrodes on a commercial textile. (b) Images of the pristine textile, the textile with 8 layers of PEDOT:PSS, and the textile with 8 layers of PEDOT:PSS and 5 layers of cholinium lactate-based iongel. (c) Electrocardiograms (ECG) data acquired under different conditions: static recoding at t_0 in the top left corner; static recording at t_0 + 40 days in the top right corner; and dynamic recording under repeated hand motion at t_0 + 40 days in the bottom center. Reprinted with permission from Bihar *et al.*[256] Copyright 2017, John Wiley and Sons.

of the iongel. Son *et al.*[260] fabricated an iongel based on PVC, [C_2mim][TFSI] IL, and dibutyl adipate (DBA). The application of this iongel material in human motion was tested by monitoring sign language and control a mouse pointer in the screen (Fig. 14).[260] Cao *et al.*[261] synthesized an iongel by entrapping [C_2mim][TFSI] into a poly(ethyl acrylate) (PEA)-based elastomer and tested it as mechanically compliant conductor for a flexible skin sensor. The transparent hydrophobic iongel exhibited elasticity of 15 – 484 kPa, ultrahigh stretchability > 5000 %, and fracture toughness up to 4.7 kJ m^{-2}. The skin-like sensor fabricated using this iongel showed remarkable durability (10,000 cycles at 100 % strain) and various motion behaviours were monitored at high vacuum (6×10^{-4} Pa), low/high temperatures (–70 and 100 ºC), and high relative humidity (99 %).[261] Furthermore, Luque *et al.*[167] fabricated a pressure sensor, containing a supramolecular iongel based on PVA, tanic acid and [Ch][Lac] IL, that was also capable to detect human motion, showing a high sensitivity (0.1 kPa^{-1}) with an excellent reversibility.

Aiming at a more sustainable and economically viable approach, Panzer and coworkers[73] fabricated DES gel materials with choline chloride (ChCl)/ethylene glycol and gelatin for the fabrication of ionic skin prototype sensor devices to monitor human finger bending and multi-touch stimuli.[73] Likewise, Hong *et al.*[262] prepared a gel-based material containing PAAM and ChCl/Urea/Glycerol. The resulting material displayed strain-sensitive of conductive elastomers and exhibited great real-time monitoring ability.

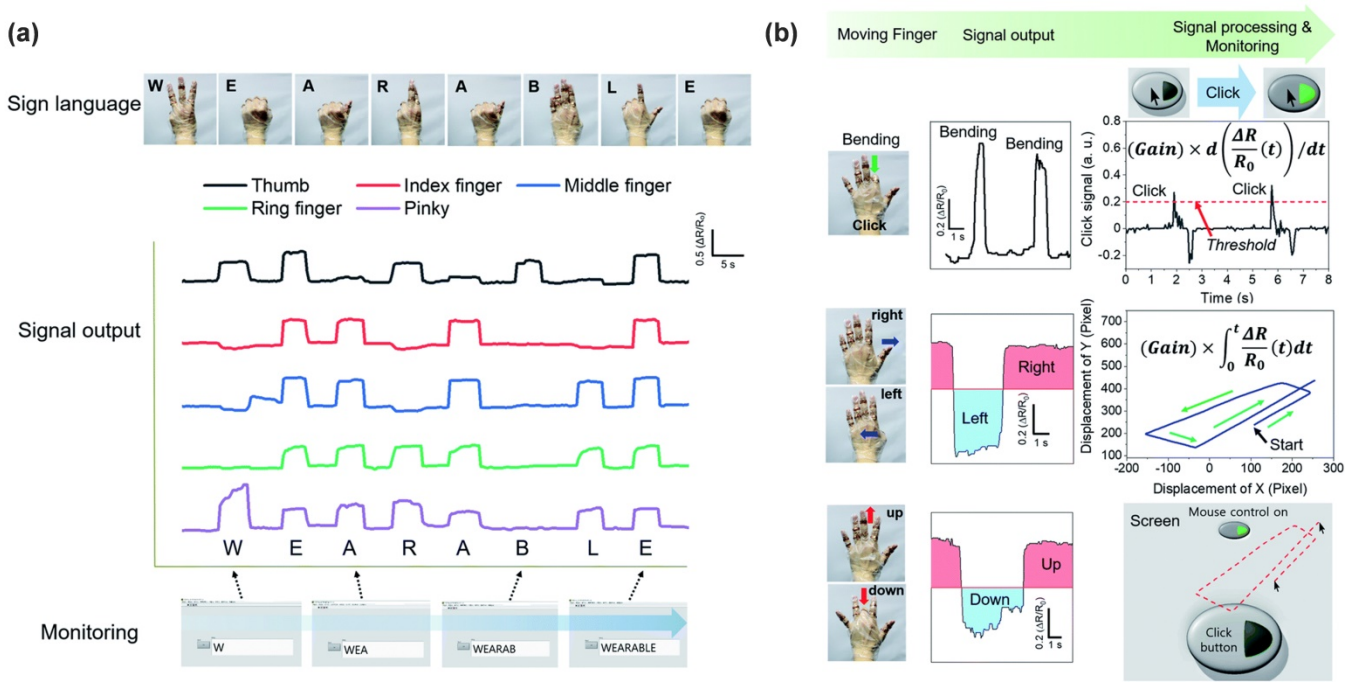

Fig. 14 Application of iongels in wearable devices (a) Transparent iongel gloves for signaling and monitoring sign language. (b) An iongel glove was used as a mouse controller. Reprinted with permission from Son *et al.*[260] Copyright 2020, Royal Society of Chemistry.

Another example is iongels that demonstrated potential for their application in electrolyte-gated organic transistors. For instance, Thiburce *et al.*[263] reported high performance electrolyte-gated organic thin-film transistors employing a PIL/IL iongel, that is, poly(DADMA TFSI)/[C_4mpyr][TFSI], as a gate insulator. The devices revealed high transconductance of 3 mS and channel current > 1 mA at operating voltages of only –1.0 V. On the other hand, Kim and coworkers,[145] recently proposed biocompatible and biodegradable organic transistors using an iongel as solid-state electrolyte, composed of levan polysaccharide and cholinium-based ILs. Owing to its electrochemical properties, namely large specific capacitance (40 μF cm^{-2} at 10 Hz), the electrolyte based organic transistors operated at low voltage range (V_{DS} = –1.0 V and V_{GS} = –2.0). This nontoxic organic transistor was also applied for electrocardiogram (ECG) recordings on human skin and the heart of a rat.[145]

Materials challenges and perspectives on iongels for bioelectronics

In summary, the device demonstrations discussed above reinforces that iongels represents a promising non-volatile alternative to hydrogels for (bio)electronics. The main conclusions and perspectives in this section are:

(1) The use of iongels in (bio)electronics is the most recent area of applications and probably the one that offers more possibilities for the future.

(2) Iongels having additional properties such as electronic conductivity, biocompatibility or biodegradability need to be developed to push the different applications and discover new ones.

(3) The use of biologically active iongels in new drug delivery devices such as ion-pumps should become one of the fields of future applications for these materials.

5. Conclusions

Nowadays, iongels cover a wide range of soft solid materials mostly composed by an IL component which can be immobilized within different matrices (polymers, inorganic networks, biopolymers, inorganic nanoparticles). Although there have been a great number of articles published relating to iongels, the emergence of alternatives to the expensive ILs, such as DES,[264, 265] still offer a lot of room for development. We provided an analysis of the main families of iongels, and highlighted the new ionic soft materials offering additional properties, such as thermoresponsiveness, self-healing, mixed ionic/electronic properties, (photo)luminescence or magnetic properties. Furthermore, recent success stories in additive manufacturing (3D printing) of iongels anticipate the future implementation of these soft ionic materials.

The applications of iongels so far were centred through the areas of energy (battery, supercapacitors, solar cells) and the area of gas separation membranes. However, most of the remaining challenges are related to the robustness of the materials and the cost/performance balance of the different technologies. On the other hand, (bio)electronics has emerged in the last years as a future field of application of iongels. In

this case, iongels having additional properties such as electronic conductivity, biocompatibility, biological activity or biodegradability, need to be developed to push the different application possibilities. All in all, this review presents an integrated perspective on the recent progress and advances in the field of emerging iongel materials.

Author Contributions

Liliana C. Tomé: conceptualization, writing – original draft, review & editing. Luca Porcarelli: writing – original draft. Jason E. Bara: writing – original draft. Maria Forsyth: review & editing. David Mecerreyes: conceptualization, supervision, writing – original draft, review & editing.

Conflicts of interest

There are no conflicts to declare.

Acknowledgements

The authors are grateful to Dr. Juan J. Torres (CONICET, Argentina) for his valuable help in editing the figures of this review. Liliana C. Tomé and Luca Porcarelli have received funding from the European Union's Horizon 2020 research and innovation programme under the Marie Sklodowska-Curie grant agreements nos. 745734 and 797295, respectively. Liliana C. Tomé is thankful to FCT (Fundação para a Ciência e a Tecnologia) in Portugal for her research contract under Scientific Employment Stimulus (2020.01555.CEECIND). Associate Laboratory for Green Chemistry – LAQV is also financed by national funds from FCT/MCTES (UIDB/50006/2020 and UIDP/50006/2020)". Jason E. Bara acknowledges support from the United States National Science Foundation (1605411) and the United States Department of Energy (DE-SC0018181). This work was supported by Marie Sklodowska-Curie Research and Innovation Staff Exchanges (RISE) project under the grant agreement no. 823989 "IONBIKE".

Abbreviations

ChCl	Choline chloride
CH_4	Methane
CO_2	Carbon dioxide
DBA	Dibutyl adipate
DES	Deep eutectic solvents
DMTA	Dynamic mechanical thermal analysis
ECG	Electrocardiography
EMG	Electromyography
EGDMA	Ethylene glycol dimethacrylate
H_2	Hydrogen
H_2S	Hydrogen sulphide
ILs	Ionic liquids
ILE	Ionic liquid electrolyte
MILs	Methacryloxy-based ionic liquid monomers
MMA	Methyl methacrylate
MOFs	Metal organic frameworks
N_2	Nitrogen
O_2	Oxygen
PA	Polyamide
PAN	Poly(acrylonitrile)
PBA	Poly(butyl acrylate)
PDMS	Poly(dimethylsiloxane)
PDADMA	Poly(diallyldimethylammonium)
PEA	Poly(ethyl acrylate)
PEO	Poly(ethylene oxide)
PEDOT	Poly(3,4-ethylenedioxythiophene)
PEGDA	Poly(ethylene glycol) diacrylate
PEGDMA	Poly(ethylene glycol) dimethacrylate
PET	Poly(ethylene terephthalate)
PI	Polyimide
PILs	Poly(ionic liquid)s
PMMA	Poly(methyl methacrylate)
PNIPAM	Poly(*N*-isopropylacrylamide)
PS	Poly(styrene)
PVA	Poly(vinyl alcohol)
PVC	Poly(vinyl chloride)
PVDF	Poly(vinylidene fluoride)
PVDF-HFP	Poly(vinylidene fluoride-co-hexafluoropropylene)
SILMs	Supported ionic liquid membranes
SLA	Stereolithography
TFC	Thin-film composite
t_{Li}	Li^+ transference number
UPy	Ureido-pyrimidinone
UV	Ultraviolet
12-HSA	12-hydroxystearic acid
$[R_nmim]^+$	1-Alkyl-3-methylimidazolium
$[R_nmpyr]^+$	1-Alkyl-3-methylpyrrolidinium
$[R_nmpip]^+$	1-Alkyl-3-methylpiperidinium
$[P_{m.n.o.p}]^+$	Tetraalkylphosphonium
$[N_{m.n.o.p}]^+$	Tetraalkylammonium
$[Ch]^+$	Cholinium
$[Br]^-$	Bromide
$[Cl]^-$	Chloride
$[TFSI]^-$	Bis(trifluoromethylsulfonyl)amide
$[FSI]^-$	Bis(fluorosulfonyl)imide
$[PF_6]^-$	Hexafluorophosphate
$[BF_4]^-$	Tetrafluoroborate
$[EtSO_4]^-$	Ethyl sulfate
$[CF_3SO_3]^-$	Trifluoromethanesulfonate
$[N(CN)_2]^-$	Dicyanamide
$[C(CN)_3]^-$	Tricyanomethanide
$[B(CN)_4]^-$	Tetracyanoborate
$[(MeO)HPO_2]^-$	Methylphosphonate
$[FeCl_4]^-$	Tetrachloroferrate
$[Ac]^-$	Acetate
$[Lac]^-$	Lactate
$[Pro]^-$	Prolinate

References

1 J. W. Steed, *Chem. Commun.*, 2011, **47**, 1379-1383.

2 L. A. Estroff and A. D. Hamilton, *Chem. Rev.*, 2004, **104**, 1201-1218.
3 P. Terech and R. G. Weiss, *Chem. Rev.*, 1997, **97**, 3133-3160.
4 M. A. B. H. Susan, T. Kaneko, A. Noda and M. Watanabe, *J. Am. Chem. Soc.*, 2005, **127**, 4976-4983.
5 J. Le Bideau, L. Viau and A. Vioux, *Chem. Soc. Rev.*, 2011, **40**, 907-925.
6 M. P. Singh, R. K. Singh and S. Chandra, *Prog. Mater Sci.*, 2014, **64**, 73-120.
7 M. Salsamendi, L. Rubatat and D. Mecerreyes, in *Electrochemistry in Ionic Liquids: Volume 1: Fundamentals*, ed. A. A. J. Torriero, Springer International Publishing, Cham, 2015, DOI: 10.1007/978-3-319-13485-7_9, pp. 283-315.
8 T. P. Lodge and T. Ueki, *Acc. Chem. Res.*, 2016, **49**, 2107-2114.
9 P. C. Marr and A. C. Marr, *Green Chem.*, 2016, **18**, 105-128.
10 N. Chen, H. Zhang, L. Li, R. Chen and S. Guo, *Adv. Energy Mater.*, 2018, **8**, 1702675.
11 H. Wang, Z. Wang, J. Yang, C. Xu, Q. Zhang and Z. Peng, *Macromol. Rapid Commun.*, 2018, **39**, 1800246.
12 N. V. Plechkova and K. R. Seddon, *Chem. Soc. Rev.*, 2008, **37**, 123-150.
13 T. L. Greaves and C. J. Drummond, *Chem. Rev.*, 2015, **115**, 11379-11448.
14 Q. Zhang, K. De Oliveira Vigier, S. Royer and F. Jérôme, *Chem. Soc. Rev.*, 2012, **41**, 7108-7146.
15 M. Forsyth, L. Porcarelli, X. Wang, N. Goujon and D. Mecerreyes, *Acc. Chem. Res.*, 2019, **52**, 686-694.
16 X. Zhang, M. Kar, T. C. Mendes, Y. Wu and D. R. MacFarlane, *Adv. Energy Mater.*, 2018, **8**, 1702702.
17 S.-Y. Lee, A. Ogawa, M. Kanno, H. Nakamoto, T. Yasuda and M. Watanabe, *J. Am. Chem. Soc.*, 2010, **132**, 9764-9773.
18 K. M. Bothwell, F. Lorenzini, E. Mathers, P. C. Marr and A. C. Marr, *ACS Sustain. Chem. Eng.*, 2019, **7**, 2686-2690.
19 F. Pena-Pereira, Ł. Marcinkowski, A. Kloskowski and J. Namieśnik, *Analyst*, 2015, **140**, 7417-7422.
20 M. G. Cowan, D. L. Gin and R. D. Noble, *Acc. Chem. Res.*, 2016, **49**, 724-732.
21 N. Joshi, K. Rawat, P. R. Solanki and H. B. Bohidar, *Sens. Biosensing. Res.*, 2015, **5**, 105-111.
22 D. Khodagholy, V. F. Curto, K. J. Fraser, M. Gurfinkel, R. Byrne, D. Diamond, G. G. Malliaras, F. Benito-Lopez and R. M. Owens, *J. Mater. Chem.*, 2012, **22**, 4440-4443.
23 P. Leleux, C. Johnson, X. Strakosas, J. Rivnay, T. Hervé, R. M. Owens and G. G. Malliaras, *Adv. Healthcare Mater.*, 2014, **3**, 1377-1380.
24 M. Petkovic, K. R. Seddon, L. P. N. Rebelo and C. Silva Pereira, *Chem. Soc. Rev.*, 2011, **40**, 1383-1403.
25 J. Hulsbosch, D. E. De Vos, K. Binnemans and R. Ameloot, *ACS Sustain. Chem. Eng.*, 2016, **4**, 2917-2931.
26 L. C. Tomé, D. J. S. Patinha, R. Ferreira, H. Garcia, C. S. Pereira, C. S. R. Freire, L. P. N. Rebelo and I. M. Marrucho, *Chemsuschem*, 2014, **7**, 110-113.
27 H. Wang, G. Gurau and R. D. Rogers, *Chem. Soc. Rev.*, 2012, **41**, 1519-1537.
28 F. Siopa, T. Figueiredo, R. F. M. Frade, I. Neto, A. Meirinhos, C. P. Reis, R. G. Sobral, C. A. M. Afonso and P. Rijo, *ChemistrySelect*, 2016, **1**, 5909-5916.
29 L. C. Tomé, N. H. C. S. Silva, H. R. Soares, A. S. Coroadinha, P. Sadocco, I. M. Marrucho and C. S. R. Freire, *Green Chem.*, 2015, **17**, 4291-4299.
30 I. M. Marrucho, L. C. Branco and L. P. N. Rebelo, *Annu. Rev. Chem. Biomol. Eng.*, 2014, **5**, 527-546.
31 M. Watanabe, M. L. Thomas, S. Zhang, K. Ueno, T. Yasuda and K. Dokko, *Chem. Rev.*, 2017, **117**, 7190-7239.
32 J. E. Bara, T. K. Carlisle, C. J. Gabriel, D. Camper, A. Finotello, D. L. Gin and R. D. Noble, *Ind. Eng. Chem. Res.*, 2009, **48**, 2739-2751.
33 A. Brandt, J. Grasvik, J. P. Hallett and T. Welton, *Green Chem.*, 2013, **15**, 550-583.
34 T. D. Ho, C. Zhang, L. W. Hantao and J. L. Anderson, *Anal. Chem.*, 2013, **86**, 262-285.
35 M. Armand, F. Endres, D. R. MacFarlane, H. Ohno and B. Scrosati, *Nat Mater*, 2009, **8**, 621-629.
36 M. G. Freire, A. F. M. Claudio, J. M. M. Araujo, J. A. P. Coutinho, I. M. Marrucho, J. N. C. Lopes and L. P. N. Rebelo, *Chem. Soc. Rev.*, 2012, **41**, 4966-4995.
37 J. Chen, F. Xie, X. Li and L. Chen, *Green Chem.*, 2018, **20**, 4169-4200.
38 Q. Yang, Z. Zhang, X.-G. Sun, Y.-S. Hu, H. Xing and S. Dai, *Chem. Soc. Rev.*, 2018, **47**, 2020-2064.
39 J. M. Gomes, S. S. Silva and R. L. Reis, *Chem. Soc. Rev.*, 2019, **48**, 4317-4335.
40 S. H. K.P, M. S. Thayyil, S. K. Deshpande, J. T.V and J. Kolte, *Solid State Ion.*, 2017, **310**, 166-175.
41 M. Li, J. Li, H. Na and J. J. Vlassak, *Soft Matter*, 2014, **10**, 7993-8000.
42 C.-W. Liew, S. Ramesh and A. K. Arof, *Int. J. Hydrogen Energy*, 2014, **39**, 2953-2963.
43 C.-W. Liew, S. Ramesh and A. K. Arof, *Int. J. Hydrogen Energy*, 2014, **39**, 2917-2928.
44 H. Cheng, X. He, Z. Fan and J. Ouyang, *Adv. Energy Mater.*, 2019, **9**, 1901085.
45 J. C. Jansen, K. Friess, G. Clarizia, J. Schauer and P. Izák, *Macromolecules*, 2011, **44**, 39-45.
46 S. Ketabi and K. Lian, *Electrochim. Acta*, 2013, **103**, 174-178.
47 J. H. Ri, J. Jin, J. Xu, T. Peng and K. I. Ryu, *Electrochim. Acta*, 2016, **201**, 251-259.
48 A. S. Shaplov, R. Marcilla and D. Mecerreyes, *Electrochim. Acta*, 2015, **175**, 18-34.
49 P. Li, D. R. Paul and T.-S. Chung, *Green Chem.*, 2012, **14**, 1052-1063.
50 T. K. Carlisle, G. D. Nicodemus, D. L. Gin and R. D. Noble, *J. Membr. Sci.*, 2012, **397–398**, 24-37.
51 M. Díaz, A. Ortiz, M. Isik, D. Mecerreyes and I. Ortiz, *Int. J. Hydrogen Energy*, 2015, **40**, 11294-11302.
52 A. J. D'Angelo and M. J. Panzer, *Adv. Energy Mater.*, 2018, **8**, 1801646.
53 K. Mathieu, C. Jérôme and A. Debuigne, *Polym. Chem.*, 2018, **9**, 428-437.

54 P. Nellepalli, L. C. Tomé, K. Vijayakrishna and I. M. Marrucho, *Ind. Eng. Chem. Res.*, 2019, **58**, 2017-2026.
55 G. B. Appetecchi, G. T. Kim, M. Montanino, M. Carewska, R. Marcilla, D. Mecerreyes and I. De Meatza, *J. Power Sour.*, 2010, **195**, 3668-3675.
56 G. A. Tiruye, D. Muñoz-Torrero, J. Palma, M. Anderson and R. Marcilla, *J. Power Sour.*, 2016, **326**, 560-568.
57 M. Brinkkötter, E. I. Lozinskaya, D. O. Ponkratov, P. S. Vlasov, M. P. Rosenwinkel, I. A. Malyshkina, Y. Vygodskii, A. S. Shaplov and M. Schönhoff, *Electrochim. Acta*, 2017, **237**, 237-247.
58 X. Wang, G. M. A. Girard, H. Zhu, R. Yunis, D. R. MacFarlane, D. Mecerreyes, A. J. Bhattacharyya, P. C. Howlett and M. Forsyth, *ACS Appl. Energy Mater.*, 2019, **2**, 6237-6245.
59 A. F. Visentin and M. J. Panzer, *ACS Appl. Mater. Inter.*, 2012, **4**, 2836-2839.
60 K. Fujii, H. Asai, T. Ueki, T. Sakai, S. Imaizumi, U.-i. Chung, M. Watanabe and M. Shibayama, *Soft Matter*, 2012, **8**, 1756-1759.
61 R. Tamate, T. Ueki, A. M. Akimoto, R. Yoshida, T. Oyama, H. Kokubo and M. Watanabe, *RSC Adv.*, 2018, **8**, 3418-3422.
62 Y. Zhong, G. T. M. Nguyen, C. Plesse, F. Vidal and E. W. H. Jager, *J. Mater. Chem. C*, 2019, **7**, 256-266.
63 M. G. Cowan, A. M. Lopez, M. Masuda, Y. Kohno, W. M. McDanel, R. D. Noble and D. L. Gin, *Macromol. Rapid Commun.*, 2016, **37**, 1150-1154.
64 Y. Ding, J. Zhang, L. Chang, X. Zhang, H. Liu and L. Jiang, *Adv. Mater.*, 2017, **29**, 1704253.
65 D. I. Mori and D. L. Gin, *Ind. Eng. Chem. Res.*, 2018, **57**, 16012-16020.
66 M. Taghavikish, S. Subianto, Y. Gu, X. Sun, X. S. Zhao and N. R. Choudhury, *Sci. Rep.*, 2018, **8**, 10918.
67 Y. He, P. G. Boswell, P. Bühlmann and T. P. Lodge, *J. Phys. Chem. B*, 2007, **111**, 4645-4652.
68 Y. He and T. P. Lodge, *Chem. Commun.*, 2007, DOI: 10.1039/b704490a, 2732-2734.
69 Y. He and T. P. Lodge, *Macromolecules*, 2008, **41**, 167-174.
70 K. Hashimoto, M. Hirasawa, H. Kokubo, R. Tamate, X. Li, M. Shibayama and M. Watanabe, *Macromolecules*, 2019, **52**, 8430-8439.
71 C. Wang, K. Hashimoto, R. Tamate, H. Kokubo, K. Morishima, X. Li, M. Shibayama, F. Lu, T. Nakanishi and M. Watanabe, *Chem. Commun.*, 2019, **55**, 1710-1713.
72 J. Demarteau, A. Fernandez de Añastro, A. S. Shaplov and D. Mecerreyes, *Polym. Chem.*, 2020, **11**, 1481-1488.
73 H. Qin, R. E. Owyeung, S. R. Sonkusale and M. J. Panzer, *J. Mater. Chem. C*, 2019, **7**, 601-608.
74 T. J. Trivedi, D. N. Srivastava, R. D. Rogers and A. Kumar, *Green Chem.*, 2012, **14**, 2831-2839.
75 C. Yin, X. Liu, J. Wei, R. Tan, J. Zhou, M. Ouyang, H. Wang, S. J. Cooper, B. Wu, C. George and Q. Wang, *J. Mater. Chem. A*, 2019, **7**, 8826-8831.
76 B. Zhang, G. Sudre, G. Quintard, A. Serghei, L. David, J. Bernard, E. Fleury and A. Charlot, *Carbohydr. Polym.*, 2017, **157**, 586-595.
77 J.-i. Kadokawa, M.-a. Murakami, A. Takegawa and Y. Kaneko, *Carbohydr. Polym.*, 2009, **75**, 180-183.
78 A. Guyomard-Lack, N. Buchtová, B. Humbert and J. Le Bideau, *Phys. Chem. Chem. Phys.*, 2015, **17**, 23947-23951.
79 S. Thiemann, S. J. Sachnov, F. Pettersson, R. Bollström, R. Österbacka, P. Wasserscheid and J. Zaumseil, *Adv. Funct. Mater.*, 2014, **24**, 625-634.
80 S. S. Silva, J. F. Mano and R. L. Reis, *Green Chem.*, 2017, **19**, 1208-1220.
81 A. Takada and J.-i. Kadokawa, *Biomolecules*, 2015, **5**, 244-262.
82 X. Chen, B. Put, A. Sagara, K. Gandrud, M. Murata, J. A. Steele, H. Yabe, T. Hantschel, M. Roeffaers, M. Tomiyama, H. Arase, Y. Kaneko, M. Shimada, M. Mees and P. M. Vereecken, *Sci. Adv.*, 2020, **6**, eaav3400.
83 A. Vioux, L. Viau, S. Volland and J. Le Bideau, *C.R. Chim.*, 2010, **13**, 242-255.
84 M.-A. Néouze, J. Le Bideau, P. Gaveau, S. Bellayer and A. Vioux, *Chem. Mater.*, 2006, **18**, 3931-3936.
85 S. A. M. Noor, P. M. Bayley, M. Forsyth and D. R. MacFarlane, *Electrochim. Acta*, 2013, **91**, 219-226.
86 S. Khurana and A. Chandra, *Solid State Ion.*, 2019, **340**, 115027.
87 A. Guyomard-Lack, J. Abusleme, P. Soudan, B. Lestriez, D. Guyomard and J. L. Bideau, *Adv. Energy Mater.*, 2014, **4**, 1301570.
88 X. Li, S. Li, Z. Zhang, J. Huang, L. Yang and S.-i. Hirano, *J. Mater. Chem. A*, 2016, **4**, 13822-13829.
89 K. Ueno, K. Hata, T. Katakabe, M. Kondoh and M. Watanabe, *J. Phys. Chem. B*, 2008, **112**, 9013-9019.
90 T. Watanabe, R. Takahashi and T. Ono, *Soft Matter*, 2020, **16**, 1572-1581.
91 S. M. Villa, V. M. Mazzola, T. Santaniello, E. Locatelli, M. Maturi, L. Migliorini, I. Monaco, C. Lenardi, M. Comes Franchini and P. Milani, *ACS Macro Lett.*, 2019, **8**, 414-420.
92 K. Ueno and M. Watanabe, *Langmuir*, 2011, **27**, 9105-9115.
93 X. Liu, B. He, Z. Wang, H. Tang, T. Su and Q. Wang, *Sci. Rep.*, 2014, **4**, 6673.
94 Z. He and P. Alexandridis, *Phys. Chem. Chem. Phys.*, 2015, **17**, 18238-18261.
95 A. Noro, Y. Matsushita and T. P. Lodge, *Macromolecules*, 2008, **41**, 5839-5844.
96 A. Wu, F. Lu, P. Sun, X. Qiao, X. Gao and L. Zheng, *Langmuir*, 2017, **33**, 13982-13989.
97 S. Chen, N. Zhang, B. Zhang, B. Zhang and J. Song, *ACS Appl. Mater. Inter.*, 2018, **10**, 44706-44715.
98 T. Zhou, X. Gao, F. Lu, N. Sun and L. Zheng, *New J. Chem.*, 2016, **40**, 1169-1174.
99 Y. Sun, Y.-Y. Ren, Q. Li, R.-W. Shi, Y. Hu, J.-N. Guo, Z. Sun and F. Yan, *Chin. J. Polym. Sci.*, 2019, **37**, 1053-1059.
100 Q. Yu, Y. Wu, D. Li, M. Cai, F. Zhou and W. Liu, *J. Colloid Interface Sci.*, 2017, **487**, 130-140.
101 X. Wu, W. Wu, Q. Wu and W. Yan, *Langmuir*, 2017, **33**, 4242-4249.
102 R. Tamate, K. Hashimoto, T. Horii, M. Hirasawa, X. Li, M. Shibayama and M. Watanabe, *Adv. Mater.*, 2018, **30**, 1802792.

103 A. Shakeel, H. Mahmood, U. Farooq, Z. Ullah, S. Yasin, T. Iqbal, C. Chassagne and M. Moniruzzaman, *ACS Sustain. Chem. Eng.*, 2019, **7**, 13586-13626.

104 D. R. MacFarlane, N. Tachikawa, M. Forsyth, J. M. Pringle, P. C. Howlett, G. D. Elliott, J. H. Davis, M. Watanabe, P. Simon and C. A. Angell, *Energ. Environ. Sci.*, 2014, **7**, 232-250.

105 P. J. Carvalho, K. A. Kurnia and J. A. P. Coutinho, *Phys. Chem. Chem. Phys.*, 2016, **18**, 14757-14771.

106 A. Fdz De Anastro, L. Porcarelli, M. Hilder, C. Berlanga, M. Galceran, P. Howlett, M. Forsyth and D. Mecerreyes, *ACS Appl. Energy Mater.*, 2019, **2**, 6960-6966.

107 Z. Dai, R. D. Noble, D. L. Gin, X. Zhang and L. Deng, *J. Membr. Sci.*, 2016, **497**, 1-20.

108 L. C. Tomé and I. M. Marrucho, *Chem. Soc. Rev.*, 2016, **45**, 2785-2824.

109 H. S. Gao, L. Bai, J. L. Han, B. B. Yang, S. J. Zhang and X. P. Zhang, *Chem. Commun.*, 2018, **54**, 12671-12685.

110 L. C. Tomé, M. Isik, C. S. R. Freire, D. Mecerreyes and I. M. Marrucho, *J. Membr. Sci.*, 2015, **483**, 155-165.

111 A. P. S. Martins, A. Fdz De Añastro, J. L. Olmedo-Martínez, A. R. Nabais, L. A. Neves, D. Mecerreyes and L. C. Tomé, *Membranes*, 2020, **10**, 46.

112 Z. Qi, N. L. Traulsen, P. Malo de Molina, C. Schlaich, M. Gradzielski and C. A. Schalley, *Org. Biomol. Chem.*, 2014, **12**, 503-510.

113 B. Ziółkowski, Z. Ates, S. Gallagher, R. Byrne, A. Heise, K. J. Fraser and D. Diamond, *Macromol. Chem. Phys.*, 2013, **214**, 787-796.

114 A. F. Visentin, S. Alimena and M. J. Panzer, *Chemelectrochem*, 2014, **1**, 718-721.

115 E. Hayashi, K. Hashimoto, M. L. Thomas, S. Tsuzuki and M. Watanabe, *Membranes*, 2019, **9**, 81.

116 X. Wang, Q. Yang, Y. Cao, J. Zhou, H. Hao, Y. Liang and J. Hao, *Chemistry – An Asian Journal*, 2016, **11**, 722-729.

117 R. Tamate, K. Hashimoto, X. Li, M. Shibayama and M. Watanabe, *Polymer*, 2019, **178**, 121694.

118 A. P. S. Brogan, C. J. Clarke, A. Charalambidou, C. N. Loynachan, S. E. Norman, J. Doutch and J. P. Hallett, *Mater. Horiz.*, 2020, **7**, 820-826.

119 A. Noro, S. Matsushima, X. He, M. Hayashi and Y. Matsushita, *Macromolecules*, 2013, **46**, 8304-8310.

120 X. Li, Q. Li, N. Lei and X. Chen, *ACS Omega*, 2019, **4**, 2437-2444.

121 A. J. D'Angelo and M. J. Panzer, *Chem. Mater.*, 2019, **31**, 2913-2922.

122 I. del Agua, D. Mantione, N. Casado, A. Sanchez-Sanchez, G. G. Malliaras and D. Mecerreyes, *ACS Macro Lett.*, 2017, **6**, 473-478.

123 B. Ziółkowski, K. Bleek, B. Twamley, K. J. Fraser, R. Byrne, D. Diamond and A. Taubert, *Eur. J. Inorg. Chem.*, 2012, **2012**, 5245-5251.

124 F. Benito-Lopez, M. Antoñana-Díez, V. F. Curto, D. Diamond and V. Castro-López, *Lab on a Chip*, 2014, **14**, 3530-3538.

125 K. Prasad, D. Mondal, M. Sharma, M. G. Freire, C. Mukesh and J. Bhatt, *Carbohydr. Polym.*, 2018, **180**, 328-336.

126 M. Tamada, T. Watanabe, K. Horie and H. Ohno, *Chem. Commun.*, 2007, DOI: 10.1039/b705060g, 4050-4052.

127 M. Czugala, C. O'Connell, C. Blin, P. Fischer, K. J. Fraser, F. Benito-Lopez and D. Diamond, *Sens. Actuators B Chem.*, 2014, **194**, 105-113.

128 A. Saruwatari, R. Tamate, H. Kokubo and M. Watanabe, *Chem. Commun.*, 2018, **54**, 13371-13374.

129 K. Lunstroot, K. Driesen, P. Nockemann, C. Görller-Walrand, K. Binnemans, S. Bellayer, J. Le Bideau and A. Vioux, *Chem. Mater.*, 2006, **18**, 5711-5715.

130 K. Lunstroot, K. Driesen, P. Nockemann, L. Viau, P. H. Mutin, A. Vioux and K. Binnemans, *Phys. Chem. Chem. Phys.*, 2010, **12**, 1879-1885.

131 Z.-L. Xie, H.-B. Xu, A. Geßner, M. U. Kumke, M. Priebe, K. M. Fromm and A. Taubert, *J. Mater. Chem.*, 2012, **22**, 8110-8116.

132 Z. Li, J. Wang, R. Hu, C. Lv and J. Zheng, *Macromol. Rapid Commun.*, 2019, **40**, 1800776.

133 G. Singh, G. Singh, K. Damarla, P. K. Sharma, A. Kumar and T. S. Kang, *ACS Sustain. Chem. Eng.*, 2017, **5**, 6568-6577.

134 T. J. Trivedi, D. Bhattacharjya, J.-S. Yu and A. Kumar, *ChemSusChem*, 2015, **8**, 3294-3303.

135 P. Guo, A. Su, Y. Wei, X. Liu, Y. Li, F. Guo, J. Li, Z. Hu and J. Sun, *ACS Appl. Mater. Inter.*, 2019, **11**, 19413-19420.

136 S. Utrera-Barrios, R. Verdejo, M. A. López-Manchado and M. Hernández Santana, *Mater. Horiz.*, 2020, **7**, 2882-2902.

137 X. Pei, H. Zhang, Y. Zhou, L. Zhou and J. Fu, *Mater. Horiz.*, 2020, **7**, 1872-1882.

138 B. Ying, Q. Wu, J. Li and X. Liu, *Mater. Horiz.*, 2020, **7**, 477-488.

139 T. Someya, Z. Bao and G. G. Malliaras, *Nature*, 2016, **540**, 379-385.

140 Y. Wang, C. Zhu, R. Pfattner, H. Yan, L. Jin, S. Chen, F. Molina-Lopez, F. Lissel, J. Liu, N. I. Rabiah, Z. Chen, J. W. Chung, C. Linder, M. F. Toney, B. Murmann and Z. Bao, *Sci. Adv.*, 2017, **3**, e1602076.

141 Z.-L. Xie, A. Jeličić, F.-P. Wang, P. Rabu, A. Friedrich, S. Beuermann and A. Taubert, *J. Mater. Chem.*, 2010, **20**, 9543-9549.

142 Z. He and P. Alexandridis, *Adv. Colloid Interface Sci.*, 2017, **244**, 54-70.

143 M. Isik, R. Gracia, L. C. Kollnus, L. C. Tomé, I. M. Marrucho and D. Mecerreyes, *ACS Macro Lett.*, 2013, **2**, 975-979.

144 A. Y. Yuen, L. Porcarelli, R. H. Aguirresarobe, A. Sanchez-Sanchez, I. Del Agua, U. Ismailov, G. G. Malliaras, D. Mecerreyes, E. Ismailova and H. Sardon, *Polymers*, 2018, **10**.

145 Y. J. Jo, H. Kim, J. Ok, Y.-J. Shin, J. H. Shin, T. H. Kim, Y. Jung and T.-i. Kim, *Adv. Funct. Mater.*, **n/a**, 1909707.

146 M. M. Villar-Chavero, J. C. Domínguez, M. V. Alonso, M. Oliet and F. Rodriguez, *Carbohydr. Polym.*, 2020, **229**, 115569.

147 Y. Wang, S. Kalytchuk, Y. Zhang, H. Shi, S. V. Kershaw and A. L. Rogach, *J. Phys. Chem. Lett.*, 2014, **5**, 1412-1420.

148 R. C. Evans and P. C. Marr, *Chem. Commun.*, 2012, **48**, 3742-3744.

149 A. C. Marr and P. C. Marr, *Dalton Trans.*, 2011, **40**, 20-26.

150 B. A. Voss, J. E. Bara, D. L. Gin and R. D. Noble, *Chem. Mater.*, 2009, **21**, 3027-3029.
151 M. Ha, W. Zhang, D. Braga, M. J. Renn, C. H. Kim and C. D. Frisbie, *ACS Appl. Mater. Inter.*, 2013, **5**, 13198-13206.
152 H. J. Kim, H. M. Yang, J. Koo, M. S. Kang, K. Hong and K. H. Lee, *ACS Appl. Mater. Inter.*, 2017, **9**, 42978-42985.
153 Y. Zhong, G. T. M. Nguyen, C. Plesse, F. Vidal and E. W. H. Jager, *ACS Appl. Mater. Inter.*, 2018, **10**, 21601-21611.
154 J. Wong, A. T. Gong, P. A. Defnet, L. Meabe, B. Beauchamp, R. M. Sweet, H. Sardon, C. L. Cobb and A. Nelson, *Adv. Mater. Technol.*, 2019, **4**, 1900452.
155 B. U. Ye, B.-J. Kim, J. Ryu, J. Y. Lee, J. M. Baik and K. Hong, *Nanoscale*, 2015, **7**, 16189-16194.
156 H. Takeno and M. Kozuka, *Adv. Mater. Sci. Eng.*, 2017, DOI: 10.1155/2017/4762379.
157 H. Nakajima and H. Ohno, *Polymer*, 2005, **46**, 11499-11504.
158 J. E. Bara, E. S. Hatakeyama, D. L. Gin and R. D. Noble, *Polym. Adv. Technol.*, 2008, **19**, 1415-1420.
159 J. Zimmermann, L. Porcarelli, T. Rödlmeier, A. Sanchez-Sanchez, D. Mecerreyes and G. Hernandez-Sosa, *Adv. Funct. Mater.*, 2018, **28**, 1705795.
160 B. Tang, D. K. Schneiderman, F. Zare Bidoky, C. D. Frisbie and T. P. Lodge, *ACS Macro Lett.*, 2017, **6**, 1083-1088.
161 J. H. Cho, J. Lee, Y. Xia, B. Kim, Y. He, M. J. Renn, T. P. Lodge and C. Daniel Frisbie, *Nat. Mater.*, 2008, **7**, 900-906.
162 K. H. Lee, M. S. Kang, S. Zhang, Y. Gu, T. P. Lodge and C. D. Frisbie, *Adv. Mater.*, 2012, **24**, 4457-4462.
163 K. G. Cho, H. J. Kim, H. M. Yang, K. H. Seol, S. J. Lee and K. H. Lee, *ACS Appl. Mater. Inter.*, 2018, **10**, 40672-40680.
164 A. Taubert, *Eur. J. Inorg. Chem.*, 2015, **2015**, 1148-1159.
165 A. R. Schultz, P. M. Lambert, N. A. Chartrain, D. M. Ruohoniemi, Z. Zhang, C. Jangu, M. Zhang, C. B. Williams and T. E. Long, *ACS Macro Lett.*, 2014, **3**, 1205-1209.
166 K. Ahmed, N. Naga, M. Kawakami and H. Furukawa, *Macromol. Chem. Phys.*, 2018, **219**, 1800216.
167 G. C. Luque, M. L. Picchio, A. P. S. Martins, A. Dominguez-Alfaro, N. Ramos, I. del Agua, B. Marchiori, D. Mecerreyes, R. J. Minari and L. C. Tomé, *Adv. Electron. Mater.*, **n/a**, 2100178.
168 A. Basu, J. Wong, B. Cao, N. Boechler, A. J. Boydston and A. Nelson, *ACS Appl. Mater. Inter.*, 2021, **13**, 19263-19270.
169 M. Isik, T. Lonjaret, H. Sardon, R. Marcilla, T. Herve, G. G. Malliaras, E. Ismailova and D. Mecerreyes, *J. Mater. Chem. C*, 2015, **3**, 8942-8948.
170 L. C. Tomé, D. Mecerreyes, C. S. R. Freire, L. P. N. Rebelo and I. M. Marrucho, *J. Mater. Chem. A*, 2014, **2**, 5631-5639.
171 M. Brachet, D. Gaboriau, P. Gentile, S. Fantini, G. Bidan, S. Sadki, T. Brousse and J. Le Bideau, *J. Mater. Chem. A*, 2016, **4**, 11835-11843.
172 E. Quartarone and P. Mustarelli, *J. Electrochem. Soc.*, 2020, **167**, 050508.
173 R. Yunis, G. M. A. Girard, X. Wang, H. Zhu, A. J. Bhattacharyya, P. Howlett, D. R. MacFarlane and M. Forsyth, *Solid State Ion.*, 2018, **327**, 83-92.
174 J. Zimmermann, S. Schlisske, M. Held, J.-N. Tisserant, L. Porcarelli, A. Sanchez-Sanchez, D. Mecerreyes and G. Hernandez-Sosa, *Adv. Mater. Technol.*, 2019, **4**, 1800641.
175 Y. Kitazawa, K. Iwata, R. Kido, S. Imaizumi, S. Tsuzuki, W. Shinoda, K. Ueno, T. Mandai, H. Kokubo, K. Dokko and M. Watanabe, *Chem. Mater.*, 2018, **30**, 252-261.
176 J. Ruiz-Olles, P. Slavik, N. K. Whitelaw and D. K. Smith, *Angew. Chem. Int. Ed.*, 2019, **58**, 4173-4178.
177 F. Wu, N. Chen, R. Chen, Q. Zhu, G. Tan and L. Li, *Adv. Sci.*, 2016, **3**, 1500306.
178 S. Ferrari, E. Quartarone, P. Mustarelli, A. Magistris, M. Fagnoni, S. Protti, C. Gerbaldi and A. Spinella, *J. Power Sour.*, 2010, **195**, 559-566.
179 L. Balo, Shalu, H. Gupta, V. Kumar Singh and R. Kumar Singh, *Electrochim. Acta*, 2017, **230**, 123-131.
180 J. R. Nair, L. Porcarelli, F. Bella and C. Gerbaldi, *ACS Appl. Mater. Inter.*, 2015, **7**, 12961-12971.
181 G. T. Kim, G. B. Appetecchi, M. Carewska, M. Joost, A. Balducci, M. Winter and S. Passerini, *J. Power Sour.*, 2010, **195**, 6130-6137.
182 M. W. Schulze, L. D. McIntosh, M. A. Hillmyer and T. P. Lodge, *Nano Lett.*, 2014, **14**, 122-126.
183 N. Goujon, T.-V. Huynh, K. j. Barlow, R. Kerr, K. Vezzù, V. Di Noto, L. A. O'Dell, J. Chiefari, P. C. Howlett and M. Forsyth, *Batteries & Supercaps*, 2019, **2**, 132-138.
184 X. Li, Z. Zhang, S. Li, K. Yang and L. Yang, *J. Mater. Chem. A*, 2017, **5**, 21362-21369.
185 X. Wang, H. Zhu, Gaetan M. A. Girard, R. Yunis, D. R. MacFarlane, D. Mecerreyes, A. J. Bhattacharyya, P. C. Howlett and M. Forsyth, *J. Mater. Chem. A*, 2017, **5**, 23844-23852.
186 M. Safa, A. Chamaani, N. Chawla and B. El-Zahab, *Electrochim. Acta*, 2016, **213**, 587-593.
187 D. Zhou, R. Liu, J. Zhang, X. Qi, Y.-B. He, B. Li, Q.-H. Yang, Y.-S. Hu and F. Kang, *Nano Energy*, 2017, **33**, 45-54.
188 B. P. Thapaliya, I. Popov and S. Dai, *ACS Appl. Energy Mater.*, 2020, **3**, 1265-1270.
189 W. Na, A. S. Lee, J. H. Lee, S. S. Hwang, S. M. Hong, E. Kim and C. M. Koo, *Electrochim. Acta*, 2016, **188**, 582-588.
190 N. Chen, Y. Dai, Y. Xing, L. Wang, C. Guo, R. Chen, S. Guo and F. Wu, *Energ. Environ. Sci.*, 2017, **10**, 1660-1667.
191 F. Wu, N. Chen, R. Chen, Q. Zhu, J. Qian and L. Li, *Chem. Mater.*, 2016, **28**, 848-856.
192 D. Kumar and S. A. Hashmi, *Solid State Ion.*, 2010, **181**, 416-423.
193 S. A. Hashmi, M. Y. Bhat, M. K. Singh, N. T. K. Sundaram, B. P. C. Raghupathy and H. Tanaka, *J. Solid State Electrochem.*, 2016, **20**, 2817-2826.
194 S. Song, M. Kotobuki, F. Zheng, C. Xu, S. V. Savilov, N. Hu, L. Lu, Y. Wang and W. D. Z. Li, *J. Mater. Chem. A*, 2017, **5**, 6424-6431.
195 V. K. Singh, Shalu, S. K. Chaurasia and R. K. Singh, *RSC Adv.*, 2016, **6**, 40199-40210.
196 V. K. Singh, S. K. Singh, H. Gupta, Shalu, L. Balo, A. K. Tripathi, Y. L. Verma and R. K. Singh, *J. Solid State Electrochem.*, 2018, **22**, 1909-1919.
197 T. C. Mendes, X. Zhang, Y. Wu, P. C. Howlett, M. Forsyth and D. R. Macfarlane, *ACS Sustain. Chem. Eng.*, 2019, **7**, 3722-3726.

198 A. Fdz De Anastro, N. Lago, C. Berlanga, M. Galcerán, M. Hilder, M. Forsyth and D. Mecerreyes, *J. Membr. Sci.*, 2019, **582**, 435-441.

199 A. Fdz De Anastro, N. Casado, X. Wang, J. Rehmen, D. Evans, D. Mecerreyes, M. Forsyth and C. Pozo-Gonzalo, *Electrochim. Acta*, 2018, **278**, 271-278.

200 M. Baloch, A. Vizintin, R. K. Chellappan, J. Moskon, D. Shanmukaraj, R. Dedryvere, T. Rojo and R. Dominko, *J. Electrochem. Soc.*, 2016, **163**, A2390-A2398.

201 L. Negre, B. Daffos, V. Turq, P. L. Taberna and P. Simon, *Electrochim. Acta*, 2016, **206**, 490-495.

202 L. Negre, B. Daffos, P. L. Taberna and P. Simon, *J. Electrochem. Soc.*, 2015, **162**, A5037-A5040.

203 P. Pazhamalai, K. Krishnamoorthy, V. K. Mariappan, S. Sahoo, S. Manoharan and S.-J. Kim, *Adv. Mater. Interfaces*, 2018, **5**, 1800055.

204 S. A. Chopade, S. So, M. A. Hillmyer and T. P. Lodge, *ACS Appl. Mater. Inter.*, 2016, **8**, 6200-6210.

205 O. Kim, K. Kim, U. H. Choi and M. J. Park, *Nat. Commun.*, 2018, **9**, 5029.

206 J. Zhang, W. Zhang, J. Guo, C. Yuan and F. Yan, *Electrochim. Acta*, 2015, **165**, 98-104.

207 J. Zhao, X. Shen, F. Yan, L. Qiu, S. Lee and B. Sun, *J. Mater. Chem.*, 2011, **21**, 7326-7330.

208 O. Winther-Jensen, V. Armel, M. Forsyth and D. R. MacFarlane, *Macromol. Rapid Commun.*, 2010, **31**, 479-483.

209 Y.-F. Lin, C.-T. Li, C.-P. Lee, Y.-A. Leu, Y. Ezhumalai, R. Vittal, M.-C. Chen, J.-J. Lin and K.-C. Ho, *ACS Appl. Mater. Inter.*, 2016, **8**, 15267-15278.

210 L.-Y. Chang, C.-P. Lee, C.-T. Li, M.-H. Yeh, K.-C. Ho and J.-J. Lin, *J. Mater. Chem. A*, 2014, **2**, 20814-20822.

211 W.-C. Yu, L.-Y. Lin, W.-C. Chang, S.-H. Zhong and C.-C. Su, *J. Power Sour.*, 2018, **403**, 157-166.

212 X. Chen, Q. Li, J. Zhao, L. Qiu, Y. Zhang, B. Sun and F. Yan, *J. Power Sour.*, 2012, **207**, 216-221.

213 D. A. Rakov, F. Chen, S. A. Ferdousi, H. Li, T. Pathirana, A. N. Simonov, P. C. Howlett, R. Atkin and M. Forsyth, *Nat. Mater.*, 2020, DOI: 10.1038/s41563-020-0673-0.

214 M. B. Shiflett and E. J. Maginn, *AlChE J.*, 2017, **63**, 4722-4737.

215 H. Z. Chen, P. Li and T.-S. Chung, *Int. J. Hydrogen Energy*, 2012, **37**, 11796-11804.

216 K. Friess, J. C. Jansen, F. Bazzarelli, P. Izák, V. Jarmarová, M. Kačírková, J. Schauer, G. Clarizia and P. Bernardo, *J. Membr. Sci.*, 2012, **415–416**, 801-809.

217 Z. Dai, L. Ansaloni, J. J. Ryan, R. J. Spontak and L. Deng, *Green Chem.*, 2018, **20**, 1391-1404.

218 L. Liang, Q. Gan and P. Nancarrow, *J. Membr. Sci.*, 2014, **450**, 407-417.

219 W. Fam, J. Mansouri, H. Li, J. Hou and V. Chen, *ACS Appl. Mater. Inter.*, 2018, **10**, 7389-7400.

220 W. Fam, J. Mansouri, H. Li and V. Chen, *J. Membr. Sci.*, 2017, **537**, 54-68.

221 J. E. Bara, D. L. Gin and R. D. Noble, *Ind. Eng. Chem. Res.*, 2008, **47**, 9919-9924.

222 J. E. Bara, R. D. Noble and D. L. Gin, *Ind. Eng. Chem. Res.*, 2009, **48**, 4607-4610.

223 L. C. Tomé, D. Mecerreyes, C. S. R. Freire, L. P. N. Rebelo and I. M. Marrucho, *J. Membr. Sci.*, 2013, **428**, 260-266.

224 L. C. Tomé, M. A. Aboudzadeh, L. P. N. Rebelo, C. S. R. Freire, D. Mecerreyes and I. M. Marrucho, *J. Mater. Chem. A*, 2013, **1**, 10403-10411.

225 R. M. Teodoro, L. C. Tomé, D. Mantione, D. Mecerreyes and I. M. Marrucho, *J. Membr. Sci.*, 2018, **552**, 341-348.

226 L. C. Tomé, D. C. Guerreiro, R. M. Teodoro, V. D. Alves and I. M. Marrucho, *J. Membr. Sci.*, 2018, **549**, 267-274.

227 A. S. L. Gouveia, L. Ventaja, L. C. Tomé and I. M. Marrucho, *Membranes*, 2018, **8**, 124.

228 A. S. L. Gouveia, E. Malcaitè, E. I. Lozinskaya, A. S. Shaplov, L. C. Tomé and I. M. Marrucho, *ACS Sustain. Chem. Eng.*, 2020, **8**, 7087-7096.

229 A. S. L. Gouveia, M. Yáñez, V. D. Alves, J. Palomar, C. Moya, D. Gorri, L. C. Tomé and I. M. Marrucho, *Sep. Purif. Technol.*, 2021, **259**, 118113.

230 A. S. Shaplov, S. M. Morozova, E. I. Lozinskaya, P. S. Vlasov, A. S. L. Gouveia, L. C. Tomé, I. M. Marrucho and Y. S. Vygodskii, *Polym. Chem.*, 2016, **7**, 580-591.

231 A. Ito, T. Yasuda, X. Ma and M. Watanabe, *Polym. J.*, 2017, **49**, 671-676.

232 A. Ito, T. Yasuda, T. Yoshioka, A. Yoshida, X. Li, K. Hashimoto, K. Nagai, M. Shibayama and M. Watanabe, *Macromolecules*, 2018, **51**, 7112-7120.

233 E. Hayashi, M. L. Thomas, K. Hashimoto, S. Tsuzuki, A. Ito and M. Watanabe, *CS Appl. Polym. Mater.*, 2019, **1**, 1579-1589.

234 M. S. Mittenthal, B. S. Flowers, J. E. Bara, J. W. Whitley, S. K. Spear, J. D. Roveda, D. A. Wallace, M. S. Shannon, R. Honee, R. Martens and D. T. Daly, *Ind. Eng. Chem. Res.*, 2017, **56**, 5055-5069.

235 K. E. O'Harra, I. Kammakakam, E. M. Devriese, D. M. Noll, J. E. Bara and E. M. Jackson, *Membranes*, 2019, **9**, 79.

236 K. E. O'Harra, I. Kammakakam, D. M. Noll, E. M. Turflinger, G. P. Dennis, E. M. Jackson and J. E. Bara, *Membranes*, 2020, **10**, 51.

237 A. Abedini, E. Crabtree, J. E. Bara and C. H. Turner, *Langmuir*, 2017, **33**, 11377-11389.

238 J. Szala-Bilnik, A. Abedini, E. Crabtree, J. E. Bara and C. H. Turner, *J. Phys. Chem. B*, 2019, **123**, 7455-7463.

239 T. K. Carlisle, W. M. McDanel, M. G. Cowan, R. D. Noble and D. L. Gin, *Chem. Mater.*, 2014, **26**, 1294-1296.

240 W. M. McDanel, M. G. Cowan, N. O. Chisholm, D. L. Gin and R. D. Noble, *J. Membr. Sci.*, 2015, **492**, 303-311.

241 K. Friess, M. Lanč, K. Pilnáček, V. Fíla, O. Vopička, Z. Sedláková, M. G. Cowan, W. M. McDanel, R. D. Noble, D. L. Gin and P. Izak, *J. Membr. Sci.*, 2017, **528**, 64-71.

242 F. Moghadam, E. Kamio and H. Matsuyama, *J. Membr. Sci.*, 2017, **525**, 290-297.

243 J. Yin, C. Zhang, Y. Yu, T. Hao, H. Wang, X. Ding and J. Meng, *J. Membr. Sci.*, 2020, **593**, 117405.

244 F. Moghadam, E. Kamio, A. Yoshizumi and H. Matsuyama, *Chem. Commun.*, 2015, **51**, 13658-13661.

245 I. Kammakakam, J. E. Bara, E. M. Jackson, J. Lertxundi, D. Mecerreyes and L. C. Tomé, *ACS Sustain. Chem. Eng.*, 2020, **8**, 5954-5965.
246 I. Kammakakam, J. E. Bara and E. M. Jackson, *CS Appl. Polym. Mater.*, 2020, **2**, 5067-5076.
247 V. A. Kusuma, M. K. Macala, J. Liu, A. M. Marti, R. J. Hirsch, L. J. Hill and D. Hopkinson, *J. Membr. Sci.*, 2018, **545**, 292-300.
248 J. Deng, J. B. Yu, Z. D. Dai and L. Y. Deng, *Ind. Eng. Chem. Res.*, 2019, **58**, 5261-5268.
249 Z. V. Singh, M. G. Cowan, W. M. McDanel, Y. Luo, R. Zhou, D. L. Gin and R. D. Noble, *J. Membr. Sci.*, 2016, **509**, 149-155.
250 C. A. Dunn, Z. X. Shi, R. F. Zhou, D. L. Gin and R. D. Noble, *Ind. Eng. Chem. Res.*, 2019, **58**, 4704-4708.
251 A. R. Nabais, A. P. S. Martins, V. D. Alves, J. G. Crespo, I. M. Marrucho, L. C. Tomé and L. A. Neves, *Sep. Purif. Technol.*, 2019, **222**, 168-176.
252 A. M. Sampaio, A. R. Nabais, L. C. Tomé and L. A. Neves, *Ind. Eng. Chem. Res.*, 2020, **59**, 308-317.
253 L. M. Robeson, *J. Membr. Sci.*, 2008, **320**, 390-400.
254 B. W. Rowe, L. M. Robeson, B. D. Freeman and D. R. Paul, *J. Membr. Sci.*, 2010, **360**, 58-69.
255 S. Huang, Y. Liu, Y. Zhao, Z. Ren and C. F. Guo, *Adv. Funct. Mater.*, 2019, **29**, 1805924.
256 E. Bihar, T. Roberts, E. Ismailova, M. Saadaoui, M. Isik, A. Sanchez-Sanchez, D. Mecerreyes, T. Hervé, J. B. De Graaf and G. G. Malliaras, *Adv. Mater. Technol.*, 2017, **2**, 1600251.
257 S. Velasco-Bosom, N. Karam, A. Carnicer-Lombarte, J. Gurke, N. Casado, L. C. Tomé, D. Mecerreyes and G. G. Malliaras, *Adv. Healthcare Mater.*, **n/a**, 2100374.
258 Y. Ren, J. Guo, Z. Liu, Z. Sun, Y. Wu, L. Liu and F. Yan, *Sci. Adv.*, 2019, **5**, eaax0648.
259 Y. Cao, Y. J. Tan, S. Li, W. W. Lee, H. Guo, Y. Cai, C. Wang and B. C. K. Tee, *Nat. Electron.*, 2019, **2**, 75-82.
260 Y. J. Son, J. W. Bae, H. J. Lee, S. Bae, S. Baik, K.-Y. Chun and C.-S. Han, *J. Mater. Chem. A*, 2020, **8**, 6013-6021.
261 Z. Cao, H. Liu and L. Jiang, *Mater. Horiz.*, 2020, **7**, 912-918.
262 S. Hong, Y. Yuan, C. Liu, W. Chen, L. Chen, H. Lian and H. Liimatainen, *J. Mater. Chem. C*, 2020, **8**, 550-560.
263 Q. Thiburce, L. Porcarelli, D. Mecerreyes and A. J. Campbell, *Appl. Phys. Lett.*, 2017, **110**, 233302.
264 J. D. Mota-Morales and E. Morales-Narváez, *Matter*, 2021, **4**, 2141-2162.
265 L. C. Tomé and D. Mecerreyes, *J. Phys. Chem. B*, 2020, **124**, 8465-8478.